ARTICLE

Check for updates

Cellular and Molecular Biology

STAT3 potentiates RNA polymerase I-directed transcription and tumor growth by activating RPA34 expression

Cheng Zhang[1], Juan Wang[1,2], Xiaoye Song[1], Deen Yu[1], Baoqiang Guo[3], Yaoyu Pang[4], Xiaomei Yin[1], Shasha Zhao[1✉], Huan Deng[1✉], Shihua Zhang[1✉] and Wensheng Deng[1✉]

BACKGROUND: Deregulation of either RNA polymerase I (Pol I)-directed transcription or expression of signal transducer and activator of transcription 3 (STAT3) correlates closely with tumorigenesis. However, the connection between STAT3 and Pol I-directed transcription hasn't been investigated.
METHODS: The role of STAT3 in Pol I-directed transcription was determined using combined techniques. The regulation of tumor cell growth mediated by STAT3 and Pol I products was analyzed in vitro and in vivo. RNAseq, ChIP assays and rescue assays were used to uncover the mechanism of Pol I transcription mediated by STAT3.
RESULTS: STAT3 expression positively correlates with Pol I product levels and cancer cell growth. The inhibition of STAT3 or Pol I products suppresses cell growth. Mechanistically, STAT3 activates Pol I-directed transcription by enhancing the recruitment of the Pol I transcription machinery to the rDNA promoter. STAT3 directly activates *Rpa34* gene transcription by binding to the *RPA34* promoter, which enhances the occupancies of the Pol II transcription machinery factors at this promoter. Cancer patients with RPA34 high expression lead to poor survival probability and short survival time.
CONCLUSION: STAT3 potentiates Pol I-dependent transcription and tumor cell growth by activating RPA34 in vitro and in vivo.

British Journal of Cancer (2023) 128:766–782; https://doi.org/10.1038/s41416-022-02098-6

BACKGROUND

Signal transducer and activator of transcription 3 (STAT3) is a member of the STAT family that regulates numerous biological processes, including cell proliferation and migration, apoptosis, angiogenesis, immunosuppression and cancer stem cell maintenance [1–3]. STAT3 can be activated by several canonical signaling pathways such as IL6/JAK, EGF/EGFR and ABL/SRC pathways [2, 4, 5]. After activation, STAT3 is phosphorylated, dimerized and translocated to the nucleus through its nuclear localization sequence, where it binds to STAT3 consensus sequences to activate transcription of its target genes [2, 6, 7]. Numerous studies have shown that STAT3 is also localized to mitochondria and regulates mitochondrial respiration by interacting with components of the electron transport chain (ETC) [8–12]. In addition to the roles in mitochondrial, another non-canonical role of STAT3 is that unphosphorylated STAT3 (uSTAT3) can enter the nucleus and bind to the GAS promoter sequence to modulate transcription [2, 13, 14]. The uSTAT3 contributes to cancer progression by increasing STAT3 transcription activity. Activation of *Stat3* gene transcription by IL-6 signaling augments uSTAT3 production, which promotes expression of *E2f1*, *Met* and *Mras* genes [15, 16]. Recently, many novel activators of STAT3, including lncRNA, miRNA, circRNA and proteins, have been identified [3, 17–25]. Some of them have been confirmed to be promising targets for anti-cancer therapy [3, 26–29]. Cai G et al reported that an inhibitor called SD-36 can act as a potent and selective degrader of STAT3 to inhibit the growth of a subset of acute myeloid leukemia by inducing cell cycle arrest [30]. Another inhibitor STAT3-IN-3 has been confirmed to repress tumor growth for breast cancer cell line 4T1 xenografted in mice by reducing proliferative activity [31]. It has been shown that constitutively activated STAT3 can promote cell proliferation by increasing the expression of CyclinD1, c-Myc and Survivin [32–34]. However, how STAT3 activation enhances cell proliferation is not fully understood.

Human RNA polymerase I (Pol I) is responsible for the synthesis of 45S pre-rRNA, which is instantly processed into 28S, 18S and 5.8S rRNA. Pol I products are essential to ribosomal assembly, protein synthesis and cell growth [35, 36]. Abnormally high levels of Pol I products have been observed in a subset of cancer tissues [37]. Pol I-directed transcription is tightly controlled by many factors, including Pol I general transcription factors, oncogenic factors, tumor suppressors, signaling pathways, chromatin modification and non-coding RNAs [38–43]. Despite massive advances in the research field of Pol I-directed transcription, the regulatory pathways and factors controlling this process remain to be

[1]School of Life Science and Health, Wuhan University of Science and Technology, Wuhan 430065, China. [2]School of Materials and Metallurgy, Wuhan University of Science and Technology, Wuhan 430081, China. [3]Department of Life Sciences, Manchester Metropolitan University, Manchester M15 6BH, UK. [4]Institute of Systems, Molecular and Integrative Biology, University of Liverpool, Liverpool L69 3GE, UK. ✉email: zhaoshasha@wust.edu.cn; denghuan@wust.edu.cn; zhangshihua@wust.edu.cn; dengwensheng@wust.edu.cn

Received: 24 May 2022 Revised: 25 November 2022 Accepted: 30 November 2022
Published online: 16 December 2022

identified. In our previous work, we showed that cytoskeletal filamin A (FLNA) silencing enhanced Pol I-directed transcription and cell proliferation [44]. Recently, RNA-seq analysis revealed that FLNA silencing reduced STAT3 mRNA expression in tumor cell lines. Whether STAT3 is associated with Pol I-dependent transcription hasn't been investigated. In this study, we showed that STAT3 functions as a positive factor in the regulation of Pol I-directed transcription and tumor cell survival and growth. We investigated the effect of an STAT3 inhibitor and Pol I-specific inhibitors on tumor cell growth in vitro and in vivo and explored the regulatory mechanisms of Pol I transcription mediated by STAT3.

MATERIALS AND METHODS

Plasmids, cells, and reagents

Three distinct DNA fragments encoding STAT3 shRNA molecules were synthesized by Sangon Biotech (Shanghai, China) and inserted downstream of the U6 promoter at the pLVU6-EGFP-Puro plasmid (Inovogen, Beijing, China). STAT3 and RPA34 cDNA fragments were inserted immediately downstream of the mCherry gene at the pLVEF1α-mCherry-Puro plasmid (Inovogen, Beijing, China). The rDNA promoter along with a piece of cDNA encoding a small fragment of 45S rRNA near the 5′ prime was loaded into the pGL3-basic reporter vector. Cell lines, including SaOS2, HeLa, 293 T and HepG2, were purchased from American Type Cell Collection (ATCC, USA) and cultured their corresponding medium supplied with 10% FBS (Thermo Scientific, USA) and 1× Penicillin/ Streptomycin (GE Healthcare, USA). After culturing 48 h, mycoplasma contamination tests were performed and STR (short tandem repeat) profiling was performed. Restriction enzymes were purchased from New England Biolab (USA). Biological reagents such as transfection and Western blot detection reagents were obtained from Thermo Scientific (USA). The chemicals used in this study were purchased from Sigma-Aldrich (Merk, Germany).

Transfection and cell line generation

Three distinct double-strand siRNA fragments that interfere with STAT3 expression were synthesized by Genewiz Co (Shuzhou, China). HeLa and HepG2 cells were cultured for 24 h in 12-well plates, transient transfection for cells in each well was performed using the mixture of 2 μL Turbofect (Thermo Scientific) and 60 pmoles siRNA (20 pmoles for each siRNA). Forty-eight hours post-transfection, STAT3 and ribosomal RNA were analyzed by Western blot and RT-qPCR, respectively. For the generation of cell lines with STAT3 knockdown or overexpression, the medium containing lentiviral particles was initially prepared by transfecting 293 T cells with 40 μg lentiviral vectors expressing STAT3 shRNA or mCherry-STAT3 and packaging vectors pH1 (30 μg) and pH2 (10 μg). The resulting medium was used for the transduction of HeLa, HepG2 and 293 T cells. Cells were selected with puromycin, and stable cell lines with STAT3 silencing and overexpression were verified by RT-qPCR and Western blot. For the generation of the cell lines concurrently expressing STAT3 shRNA and mCherry-RPA34, lentiviral particles expressing mCherry-STAT3 were used for the transduction of the STAT3-depleted cell lines, and the rest of the protocol followed the procedures as described above.

Endogenous protein activation and repression assays mediated by CRISPR dCas9-KRAB/VP48 and STAT3 inhibitor assays

Two DNA fragments encoding the guide RNA molecules targeting different positions at the *STAT3* promoter were synthesized by Sangon (Shanghai, China) and inserted downstream of the U6 promoter at the pLVU6-sgRNA-hUbC-dCas9-KRAB vector (Cat No. 71236, Addgene, USA) or the pAC2-dual-dCas9VP48-sgExpression vector (Cat No. 48236, Addgene, USA). The resulting vectors were transiently transfected into HepG2 cells; after 48 h, cells were harvested, and STAT3 and ribosomal RNA were detected by Western blot and RT-qPCR, respectively. For the assays with a STAT3 inhibitor, two groups of HeLa or HepG2 cells were cultured for 24 h before the STAT3 inhibitor was added into one group of cells at a final concentration of 2 μM, meanwhile, DMSO was added into another group of cells. After 48 h, STAT3 expression and phosphorylation were analyzed by Western blot using an anti-STAT3 antibody (CST#9139, CST, USA) and an anti-p-STAT3 antibody (CSB-PA004932LA01HU, CUSABio, China), while ribosomal RNA expression was detected by RT-qPCR.

Immunofluorescence assays

HeLa or HepG2 cells were cultured on small round coverslips (14 mm in diameter) in the complete medium. When growing up to 60% of culturing surface, cells were fixed for 10 min with 4% formaldehyde freshly prepared with 1× PBS solution. After fixation, immunofluorescence (IF) assays were performed as described previously [45] using the antibodies against STAT3, RPA34 (CSB-PA006734, CUSABio, China) and nucleolar protein markers (Fibrillarin, Ab66630, Ab4566, Abcam, UK). IF assays for HepG2 cell lines expressing STAT3 shRNA or control shRNA were performed using antibodies against RPA34 and Fibrillarin. Cell specimens were observed under a confocal fluorescence microscope, and images were captured with a 60× objective lens (Olympus). The resulting images were analyzed with ImageJ software (NIH).

RT-qPCR and 5-ethynyl uridine assays

HeLa and HepG2 cell lines expressing STAT3 shRNA or mCherry-STAT3 and their control cell lines were cultured in 6-well plates using their corresponding culture medium. At 90% confluence, cells were harvested and total RNA was extracted from the cells using an RNA extraction kit (Axygen). The expression of both *STAT3* and ribosomal RNA genes was analyzed by RT-qPCR as described previously [44, 45]. For 5-ethynyl uridine (EU) assays, HeLa or HepG2 cells were cultured and labeled with EU for 2 h; after labeling, cells were fixed with a 4 % formaldehyde solution and EU-labeled cells were detected using the Cell-Light EU Apollo 555 (or 488) Imaging Kit (RiboBio, Guangzhou). Cell samples were observed under a confocal fluorescence microscope (Olympus, Japan), and images were captured with a 20×objective lens. The fluorescence intensity for nucleoli or nucleoplasm area was obtained with the Image J software. The relative fluorescence intensity for a nucleolus was obtained using the following formula: (the fluorescence intensity of a nucleolus − the fluorescence intensity of the equal area of nucleoplasm) × the rate of Pol I products in total rRNA (0.983). The data from EU assays were analyzed by ImageJ and Graphpad Prism 8 software.

Dot blotting

HepG2 cell lines expressing STAT3 shRNA or meCherry-STAT3 and the corresponding control cell lines were cultured in 10 cm dishes. At 90% confluence, cells were harvested and nuclei were purified from the cells. Next, total RNA was extracted from nuclei using an RNA extraction kit (Axygen). One microgram of total RNA was loaded in individual circles on a piece of nylon membrane (5 cm × 8 cm), and the membrane was dried at 65 °C for 0.5 h. Probes were prepared in a 40 μL reaction mixture containing 10 U of Klenow enzyme; 25 pmol of biotin-labeled random hexamer primers and 500 ng of template DNA amplified from the introns of 45S pre-rRNA. Dot blot hybridization was performed using standard procedures. After hybridization, the membrane was incubated for 1 h in a 5% skimmed milk-PBS solution containing 1 μL of an anti-biotin HRP-linked antibody and was washed twice with 1 ×PBS and detected with ECL reagent.

Cell proliferation assays

Cell proliferation assays for HeLa and HepG2 cell lines expressing STAT3 shRNA or mCherry-STAT3 were performed using different approaches, including cell counting, CCK8, EdU and colony formation. Cell counting, CCK-8 and EdU assays were performed as described previously [46, 47]. For colony formation, cell lines expressing STAT3 shRNA or mCherry-STAT3 and their corresponding control cell lines were diluted and seeded in 6-well plates. After culturing for 10 days, cell colonies were fixed and then stained for 15 min with 0.02% crystal violet. After that, cell samples were washed, air-dried and photographed with a camera. The number of total colonies and the sizes of individual colonies were calculated and analyzed statistically. For the analysis of cell proliferation and colony formation under the treatment with DMSO, STAT3-IN-3 (500 nM), CX-5461 (50 nM), and both STAT3-IN-3 (500 nM) and CX-5461 (50 nM), experimental procedures were the same as the assays without drug treatment described above.

Animal models for tumor formation

Sixteen of five-week-old BALB/c female nude mice were obtained from the Vital River Laboratory Animal Technology Co. (Beijing, China). The nude mice inhabited a room under a sterile condition with controlled temperature, humidity and light. After adapting for one week, mice were randomly distributed into two groups ($n = 8$ for each group). Each mouse

was subcutaneously injected using 1×10^7 HepG2 cells expressing STAT3 shRNA or control shRNA. After 7 days, growing tumors were measured with a Vernier calliper every 3 days. Tumor volumes were calculated using the formula: $V = \frac{\pi}{6} \times \text{length} \times \text{width}^2$. At the end of the sixth week, mice bearing a tumor were euthanized under the Animal Welfare Guideline, and the tumors within the mice were removed, weighed, and photographed. Tumor samples randomly picked from controls or treatments were subjected to hematoxylin and eosin (H&E) staining and immunohistochemistry analysis as described previously [48, 49]. For the tumor formation assays under the treatment with different drugs, 24 nude mice were nurtured for 1 week at a sterilized condition. After that, the mice were subcutaneously injected with 1×10^7 HepG2 cells. Five days later, mice were randomly divided into 4 groups ($n = 6$ for each group), which were injected with different drugs, including 100 µL 0.9% NaCl, 100 µL STAT3-IN-3 (3 mM), 100 µL CX-5461 (3.9 mM) and both of STAT3-IN-3 (100 µL, 3 mM) and CX-5461 (100 µL, 3.9 mM). Drug injection was carried out every 2 days until mice were euthanized. Tumor sizes and weight were analyzed as described above. Animal experiments for drug inhibitors were clearly labeled without blinding. Mouse model experiments were approved by the Animal and Medical Ethics Committee in the School of Life Science and Health at Wuhan University of Science and Technology. All animal experiments were conducted according to the Animal Welfare Guidelines (China).

Messenger RNA-seq analysis

HepG2 cell lines expressing STAT3 shRNA or control shRNA were cultured in 10-cm dishes in triplicates. At 85% confluence, cells were harvested and total RNA was extracted with a Qiagen RNeasy kit and sent to Frasergen Gene Information Co. (Wuhan, China) for mRNA-seq analysis. RNA libraries were constructed and loaded on a Novaseq 6000 instrument according to the manufacturer's instructions (Illumina, San Diego, USA). DNA sequencing was performed using a 2×150 bp paired-end (PE) configuration and sequence data were obtained by the HiSeq Control Software (HCS) + OLB + GAPipeline-1.6 (Illumina). The raw data containing adapter, PCR primers and other fragments less than 20 bases were trimmed with Trimmomatic (v0.30) so that high-quality clean data were achieved. The clean data were aligned to the human reference genome (Hg38) using software Hisat2 (v2.0.1). Differential expression analysis was performed using the DESeq Bioconductor package. GO-TermFinder was used to identify Gene Ontology (GO) terms that annotate a list of enriched genes where their *P*-values were less than 0.05. Computer codes for the volcano plotting of DEGs and dot plot for pathway enrichment analysis were stored in laboratory computer and are available on request. The upstream analysis for the RNA-seq data was performed by Frasergen Gene Information Co.

Western blot

HeLa and HepG2 cells including control or treatment cells (knockdown and overexpression) were cultured in 6-well plates. At 90% confluence, cells were harvested and lysed with 200 µL of 1× SDS loading buffer (50 mM Tris-HCl, 2% SDS, 0.1% Bromophenol blue, 10% Glycerol, 100 mM DTT). After boiling for 10 min at 100°C within a heat block, 10 µL samples were used for Western blot analysis using the antibodies against STAT3 (CST#9139, CST, USA), UBF (ab244287, Abcam, UK), TBP (SC-421, Santa Cruz Biotech, USA), TAF1A (SC-393600, Santa Cruz Biotech, USA), RPA34 (CSB-PA004932LA01HU, CUSABio, China) and RPA49 (CSB-PA050039, CUSABio, China).

Reporter assays and chromatin immunoprecipitation assays

Reporter assays were performed as described previously [45] using HeLa or HepG2 cell lines expressing STAT3 shRNA and their control cell lines, where the reporter vectors driven by the RPA34 promoter and the β-galactase-expressing vectors were co-transfected into these cell lines. For ChIP assays, HepG2 cells or HepG2 cell lines stably expressing STAT3 shRNA or control shRNA were cultured in 10-cm dishes, fixed with 10 mL 1% formaldehyde-containing PBS solution and harvested for chromatin immunoprecipitation (ChIP) analysis. ChIP assays were performed using the protocol described previously [44] except that antibodies for ChIP assays were replaced. The DNA from each ChIP assay was eluted with 40 µL ddH_2O after chromatin de-crosslinking and DNA purification, and 1 µL of ChIP DNA sample was used for a qPCR reaction, where 0.5 ng genomic DNA (0.02% input) acted as a positive control in the assay. Relative enrichment was obtained by calculating the percentage for the relative quantity of promoter DNA from 1/40 ChIP DNA samples in that from 0.02% input.

Pearson' correlation, Kaplan–Meier Plotting and Statistical analysis

Pearson correlation analysis between STAT3 and RPA34 expression in normal tissues or clinical cancer samples based on the dataset deposited at The Cancer Genome Atlas (TCGA) was performed using the GEPIA online tool (http://gepia2.cancer-pku.cn/#index). Kaplan–Meier Plotting showing the relationship between RPA34 expression levels and survival probability or survival time was performed using the Kaplan–Meier Plotter online tools (www.kmplot.com) and the RNA-seq data of liver hepatocellular carcinomas (LIHC) and kidney renal carcinoma (KIRC) deposited at the TCGA. Violin plots were obtained by Graphpad Prism 8 based on the expression data of cancer samples deposited at the TCGA.

The experiments in this study, including RT-qPCR, proliferation assays, ChIP assays and reporter assays, were carried out with the samples of three biological replicates or three independent experiments at least. All data generated in the experiments were used for statistical analysis without exclusion. The means, standard deviations (SD) and histograms for the data of cell proliferation, tumor growth, RT-qPCR, luciferase assays, and ChIP assays were calculated with the GraphPad Prism 8.0 software. *P* values were obtained by student's *t* test or two-way ANOVA wherever it is appropriate.

RESULTS

STAT3 acts as a positive factor to regulate Pol I-directed transcription

It has been shown that cytoskeletal FLNA silencing can stimulate Pol I-directed transcription [44]. Recently, we performed RNA-seq analysis using FLNA-depleted cell line (SRA accession number: SRP318361, https://www.ncbi.nlm.nih.gov/Traces/study/?acc=PRJNA726417) and found that FLNA silencing reduced the expression of both STAT3 mRNA and protein (Supplementary Fig. S1). In addition, transcription factor STAT3 has been shown to regulate cell proliferation, which is associated with Pol I product levels. Based on this information, we hypothesized that STAT3 maybe is required for the regulation of Pol I-directed transcription. To support this hypothesis, we determined the effect of STAT3 expression change on the synthesis of Pol I products in SaOS2 cells. Unexpectedly, STAT3 siRNA transfection reduced Pol I product expression rather than stimulating this process in SaOS2 cells (Supplementary Fig. S2A, B). Consistent results were obtained when similar assays were performed using HeLa and HepG2 cells (Supplementary Fig. S2C–F). These results suggest that STAT3 is required for normal transcription directed by Pol I and possibly plays a positive role in this process. This result is opposite to that observed in Supplementary Fig. S1, where FLNA knockdown reduced the expression of STAT3 (Supplementary Fig. S1) and stimulated the synthesis of Pol I products (44). To clarify the role of STAT3 in Pol I-dependent transcription, we generated several cell lines (HepG2, HeLa, 293T) stably expressing STAT3 shRNA or control shRNA (Fig. 1a, Supplementary Fig. S2G, I). However, we failed to get the SaOS2 cell line stably expressing STAT3 shRNA. The reason for this outcome is because SaOS2 cells grew extremely slow and many cells died after STAT3 silencing. Analysis of rRNA expression by RT-qPCR showed that STAT3 shRNA stable expression significantly reduced the synthesis of Pol I products (Fig. 1b, Supplementary Fig. S2H, J), indicating that STAT3 expression positively correlates with Pol I-directed transcription.

To validate the positive role of STAT3 in Pol I-directed transcription, we prepared several cell lines (HepG2, HeLa, 293 T) stably expressing mCherry-STAT3 and analyzed the effect of STAT3 overexpression on rRNA synthesis. Evidently, STAT3 overexpression enhanced the synthesis of Pol I products in these cell lines (Fig. 1c, d, Supplementary Fig. S3A–D). Since 5-ethynyl uridine (EU) can be incorporated into the RNA newly synthesized, we next examined the effect of STAT3 expression alteration on rRNA synthesis by performing EU assays using HeLa and HepG2 cell lines established above. Noticeably, STAT3 silencing reduced nucleolar fluorescence intensity (Fig. 1e, f, Supplementary Fig. S2K, L). In contrast, STAT3 overexpression augmented nucleolar fluorescence intensity when compared to control cell lines (Fig. 1g,

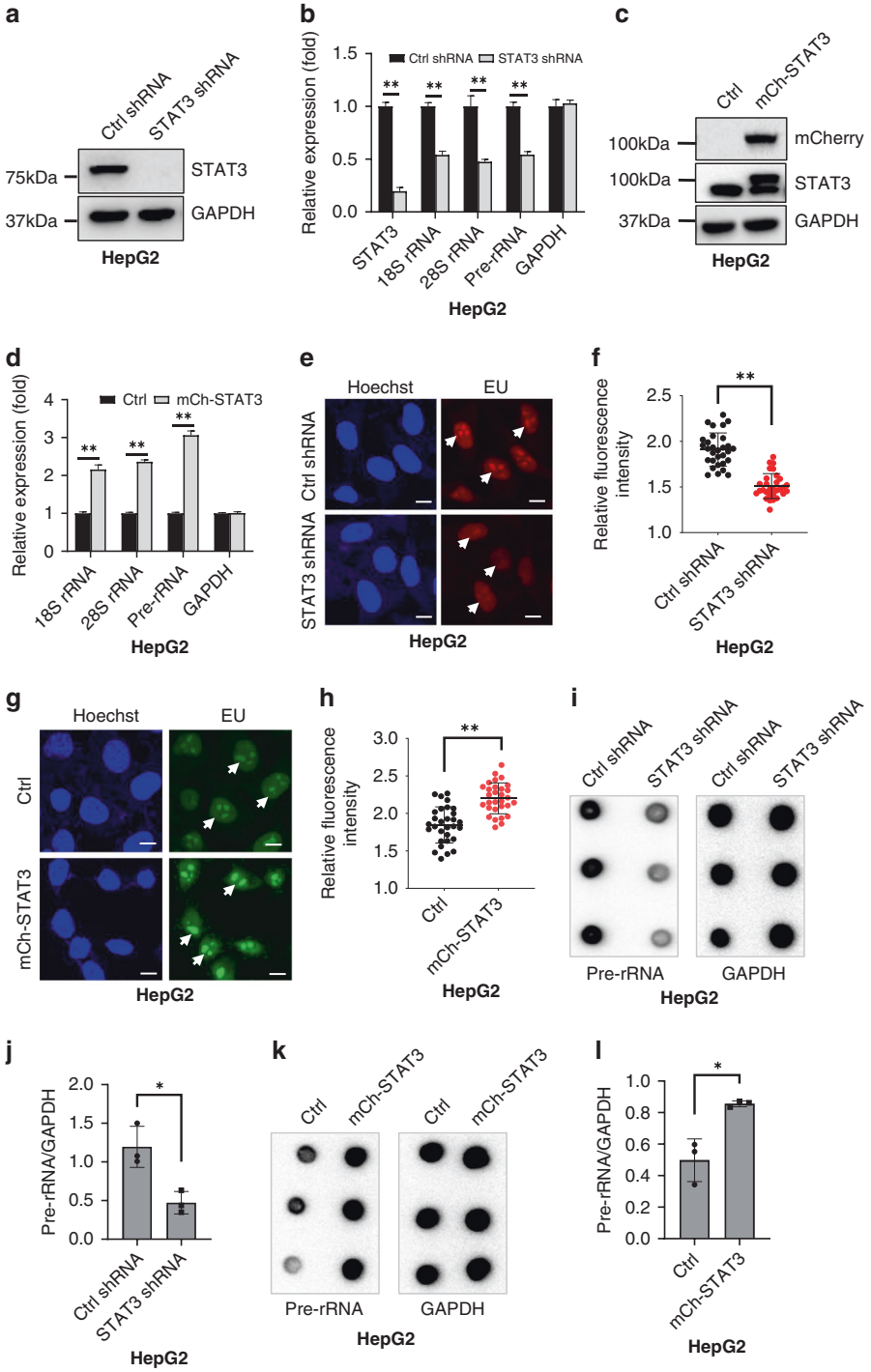

Fig. 1 Alteration of STAT3 expression affected Pol I-directed transcription. a, **b** STAT3 shRNA stable expression reduced Pol I-directed transcription in HepG2 cell lines. STAT3 expression was detected by Western blot (**a**), while Pol I products were detected by RT-qPCR (**b**). **c**, **d** mCherry-STAT3 stable expression enhanced Pol I-directed transcription in HepG2 cells. mCherry-STAT3 (**c**) and Pol I products (**d**) were analyzed by Western blot and RT-qPCR, respectively. **e**, **f** EU assay results for HepG2 cells with STAT3 silencing. EU assays were performed using the cell lines as indicated, and images were captured under a confocal fluorescence microscope (**e**). The scale bars in the images represent 5 μm. Relative fluorescence intensity for nucleoli in the images was calculated using ImageJ software (**f**). **g**, **h** EU assay results for HepG2 cells with STAT3 overexpression. EU assays were performed using the cell lines as indicated. Images (**g**) and relative fluorescence intensity for nucleoli (**h**) were obtained as described in **e** and **f**. **i**, **j** Dot blot results for the expression of pre-rRNA in HepG2 cell lines expressing STAT3 shRNA or control shRNA. **j** represents the quantified result for the dot blots obtained in **i**. **k**, **l** Dot blot results for the expression of pre-rRNA in a HepG2 cell line expressing mCherry-STAT3 (mCH-STAT3) or its control cell line. **k** represents the quantified result for the dot blots obtained in **l**. Each column in histograms represents the mean ± SD of three independent experiments ($n = 3$). *$P < 0.05$; **$P < 0.01$. P values were obtained by Student's t test, performed with control and treatment groups.

h, Supplementary Fig. S3E, F). Next, we verified these results using a more direct method (Dot blot). The results from Dot blot assays showed that STAT3 silencing reduced the synthesis of pre-rRNA (Fig. 1i, j). Conversely, STAT3 overexpression enhanced this process (Fig. 1k, l). Collectively, these results indicate that STAT3 plays a positive role in the regulation of Pol I-directed transcription in tumor cells.

Both CRISPR dCas9 activation or repression systems and a STAT3 inhibitor confirmed the positive role of STAT3 in Pol-I directed transcription

In order to gain further evidence to support that STAT3 functions as a positive factor in Pol I-mediated transcription, we utilized the CRISPR dCas-9 systems to activate or inhibit endogenous STAT3 expression and observed the effect of STAT3 activation or inhibition on rRNA synthesis. We show that endogenous STAT3 inhibition dampened the synthesis of Pol I products (Fig. 2a–c), while endogenous STAT3 activation enhanced the expression of Pol I products (Fig. 2d–f). Previous studies showed that STAT3 has to be phosphorylated before entering a nucleus [2]; STAT3-IN-3 can impede the phosphorylation of STAT3 at its Tyr^{705} and Ser^{727} sites [31], which is required for the entry of STAT3 into nuclei. Thus, we determined the effect of STAT3-IN-3 on Pol I-dependent transcription in HeLa or HepG2 cells cultured in the medium containing 5 μmol/L of STAT3-IN-3. Interestingly, the presence of STAT3-IN-3 did not affect STAT3 expression but downregulated STAT3 phosphorylation levels and the synthesis of Pol I products in both HeLa and HepG2 cells (Fig. 2g–j), suggesting that STAT3 phosphorylation is required for Pol I-directed transcription. STAT3 and Pol I products have an abnormally high expression in a subset of cancer types [1, 2, 37]. Thus, we next determined whether the expression of STAT3 and Pol I products in HeLa and HepG2 cells is higher than that in their corresponding normal cell lines using Western blot and RT-qPCR techniques. As expected, HeLa and HepG2 cells showed higher levels of STAT3 and Pol I products than their normal cell lines, including HUCEC and HL-7702 cells (Fig. 2k, l, Supplementary Fig. S4). These results further confirmed that STAT3 functions as a positive regulator in Pol I-dependent transcription in human cancer cells.

STAT3 may regulate tumor cell growth in vitro and in vivo by affecting Pol I-directed transcription

Because STAT3 expression change affected Pol I product synthesis, and Pol I product levels correlate closely with cell growth [35, 36]; it is necessary to determine the effect of STAT3 upregulation or downregulation on cell proliferation. To this end, the proliferative activity of several cell lines, including HeLa, HepG2 and 293T cell lines with STAT3 depletion or overexpression, was initially analyzed by cell counting and CCK-8 methods. Apparently, STAT3 silencing reduced cell proliferative activity for these cell lines (Fig. 3a, b, Supplementary Fig. S5A–D). In contrast, STAT3 overexpression enhanced cell proliferative activity (Fig. 3c, d, Supplementary Fig. S6 A–D). The incorporation of 5-ethynyl-2′-deoxyuridine (EdU) into genomic DNA is widely utilized to assess the activity of cell proliferation. EdU assays showed that STAT3 downregulation reduced the rate of EdU positive cells, while STAT3 overexpression augmented the rate of EdU-labeled cells (Fig. 3e–h, Supplementary Figs. S5E, F and S6E, F). Consistent results were obtained using HepG2 cells with endogenous STAT3 inhibition or activation by a dCas-9 system (Supplementary Figs. S5G, H and S6G, H). To further understand how STAT3 expression alteration affects cancer cell growth, we performed colony formation assays using HepG2 cell lines with STAT3 depletion or overexpression. Analysis of the colony number and size revealed that STAT3 downregulation reduced the number of total colonies and the sizes of individual colonies (Supplementary Fig. S7A–C), while STAT3 overexpression enhanced them (Supplementary Fig. S7D–F). These data suggest that STAT3 promotes cell growth by reducing cell death and increasing proliferative activity. We showed that STAT3 can concurrently promote cell proliferation and activate Pol I product synthesis. Therefore, we determined whether the increase of Pol I products induced by STAT3 overexpression contributes to the promotion of cell proliferation. Cell proliferation assays were performed in the presence and absence of CX-5461 (a Pol I transcription inhibitor) using HeLa and HepG2 cell lines stably expressing mCherry-STAT3. Strikingly, the presence of CX-5461 inhibited the enhancement of cell proliferation and the activation of Pol I-directed transcription induced by STAT3 overexpression (Fig. 3i, j, Supplementary Fig. S8). These data indicate that the increase of Pol I products contributes to the promotion of cell proliferation induced by STAT3 overexpression although the contribution of other pathways cannot be excluded.

To understand if alteration of Pol I products by STAT3 silencing affects cell growth in vivo, we performed tumor formation assays using nude mice ($n = 8$ for each group) subcutaneously injected with 1×10^7 HepG2 cells stably expressing STAT3 shRNA or control shRNA. Analysis of tumor sizes and weights showed that the tumors with STAT3 silencing showed the reduction in sizes and weights compared to those without STAT3 silencing (Fig. 4a–c). Further assays revealed that tumor tissues formed in nude mice possessed the morphology of liver cancer tissues (Fig. 4d) and retained the original features of HepG2 cells before injection (Fig. 4e–g). These data indicate that STAT3 silencing can inhibit tumor growth in vivo, which is associated with the reduction of Pol I products.

The presence of both STAT3-IN-3 and CX-5461 shows additive effect on the inhibition of tumor cell growth in vitro and in vivo

STAT3-IN-3 has been reported to suppress breast cancer cell growth [31]. Thus, we next evaluated the effect of STAT3-IN-3 on the proliferative activity of HeLa and HepG2 cells. Notably, the presence of STAT3-IN-3 repressed the proliferative activity of these two cell types (Fig. 5a, b, Supplementary Fig. S9). Since the presence of CX-5461 (a Pol I-specific inhibitor) suppresses the proliferation activity of HeLa and HepG2 cells (Fig. 3i, j, Supplementary Fig. S8), we next investigated whether the combination of STAT3-IN-3 and CX-5461 can cause greater inhibition to cell proliferation than the application of a single drug. Interestingly, the treatments with both CX-5461 and STAT3-IN-3 showed greater inhibition to HepG2 cell proliferation than the treatments with CX-5461 or STAT3-IN-3 (Fig. 5c, d). Whether the combination of STAT3-IN-3 and other Pol I inhibitors such as actinomycin D and BMH-21 can cause the same effect as observed above is unclear. Thus, HepG2 cells were treated with STAT3-IN-3 and actinomycin D (or BMH-21); and the results confirmed that the treatments with two drugs still showed additive effect on cell growth compared to the treatments with one drug (Supplementary Fig. S10A–D). Next, we determined how these drugs inhibit cell growth by initially analyzing expression of a cell proliferation marker (CDKN1B) and apoptosis related factors (Caspas-3 and cleaved Caspase-3) in HepG2 cells by Western blot. The treatments with both STAT3-IN-3 and CX-5461 increased expression of CDKN1B and cleaved caspase-3 and reduced expression of Caspase-3; however, the treatments with a single drug had little effect on expression of these proteins (Supplementary Fig. S10E, F), suggesting that these two drugs may inhibit cell growth by affecting cell proliferation and apoptosis. To verify this result, we performed colony formation assays; and the results showed that all treatments with drugs reduced the number of total colonies and the sizes of individual colonies compared to the DMSO treatment, indicating that both inhibitors can induce cell death and inhibit cell proliferation. Furthermore, the treatments with both CX-5461 and STAT3-IN-3 showed greater inhibition to the number and sizes of colonies than the treatments with a single

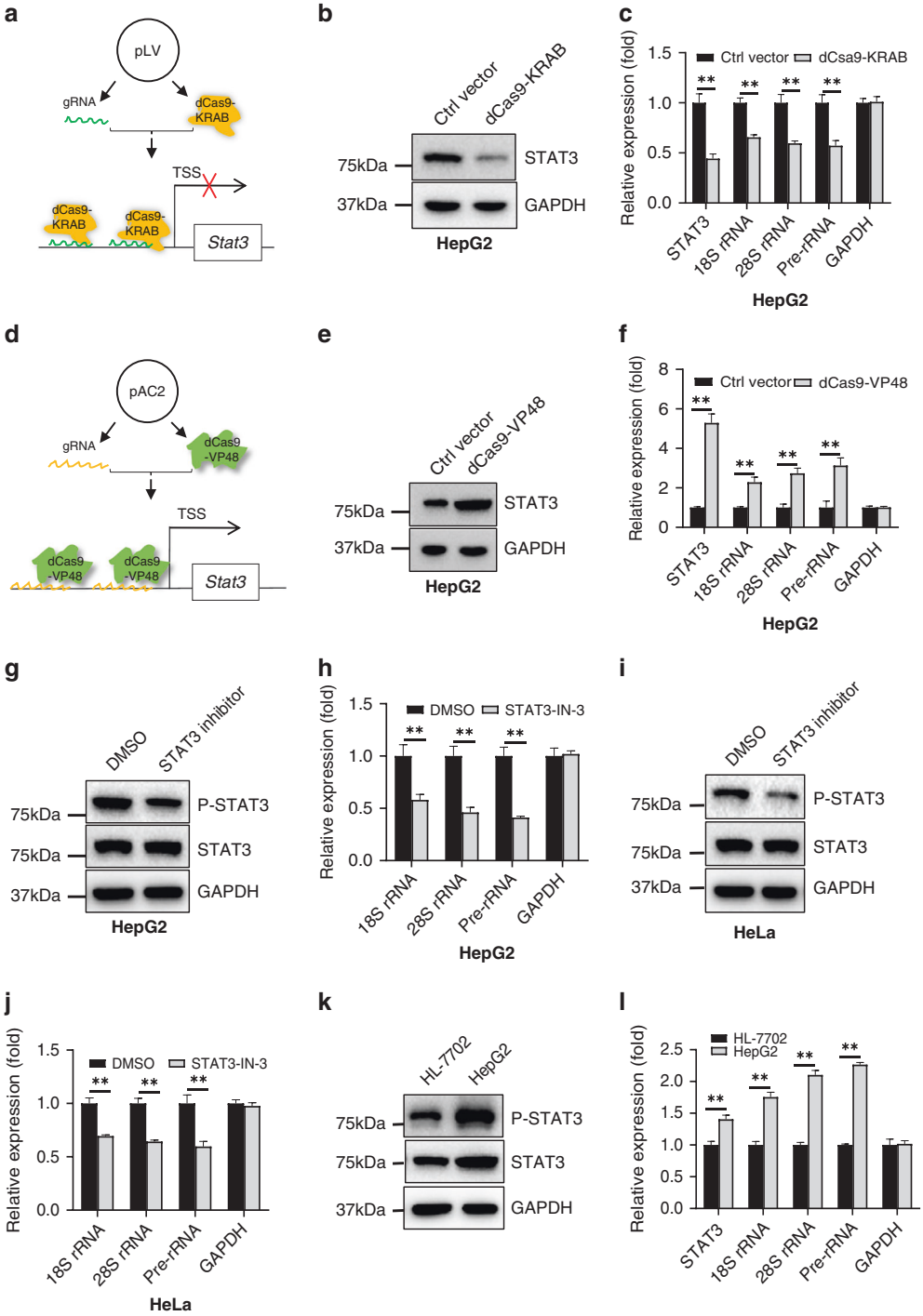

Fig. 2 The positive role of STAT3 in Pol I-directed transcription was confirmed by a dCas9 activation and repression system as well as a STAT3 inhibitor. **a** A scheme showing the guide RNA (gRNA) and dCas9-KRAB that target the *STAT3* promoter region. **b** STAT3 immunoblotting analysis in HepG2 cells transfected with the vectors expressing both STAT3 gRNAs and dCas9-KRAB or dCas9-KRAB only. **c** Analysis of Pol I products by RT-qPCR using the cells obtained in **b**. **d** A scheme showing the guide RNA (gRNA) and dCas9-VP48 that target the *STAT3* promoter region. **e** STAT3 expression analysis in HepG2 cells transfected with the vectors expressing both STAT3 gRNAs and dCas9-VP48 or dCas9-VP48 only by Western blot. **f** Detection of Pol I products by RT-qPCR using the cells obtained in **e**. **g** Analysis of STAT3 expression and phosphorylation by Western blot using HepG2 cells in the presence or absence of STAT3-IN-3 (2 μM). **h** The presence of STAT3 inhibitor reduced Pol I product expression in HepG2 cells. **i** Analysis of STAT3 expression and phosphorylation by Western blot using HeLa cells cultured in the medium with or without STAT3-IN-3 (2 μM). **j** The presence of STAT3 inhibitor inhibited Pol I product expression in HeLa cells. **k** Analysis of STAT3 expression and phosphorylation by Western blot using HepG2 cells and its primary (normal) cells (HL-7702). **l** Comparison of Pol I product levels between HL-7702 and HepG2 cells. Pol I products in **h**, **j** and **l** were detected by RT-qPCR. Each column in histograms represents the mean ± SD of three independent experiments ($n = 3$). $^{*}P < 0.05$; $^{**}P < 0.01$. P values were obtained by Student's t test, performed with control and treatment groups.

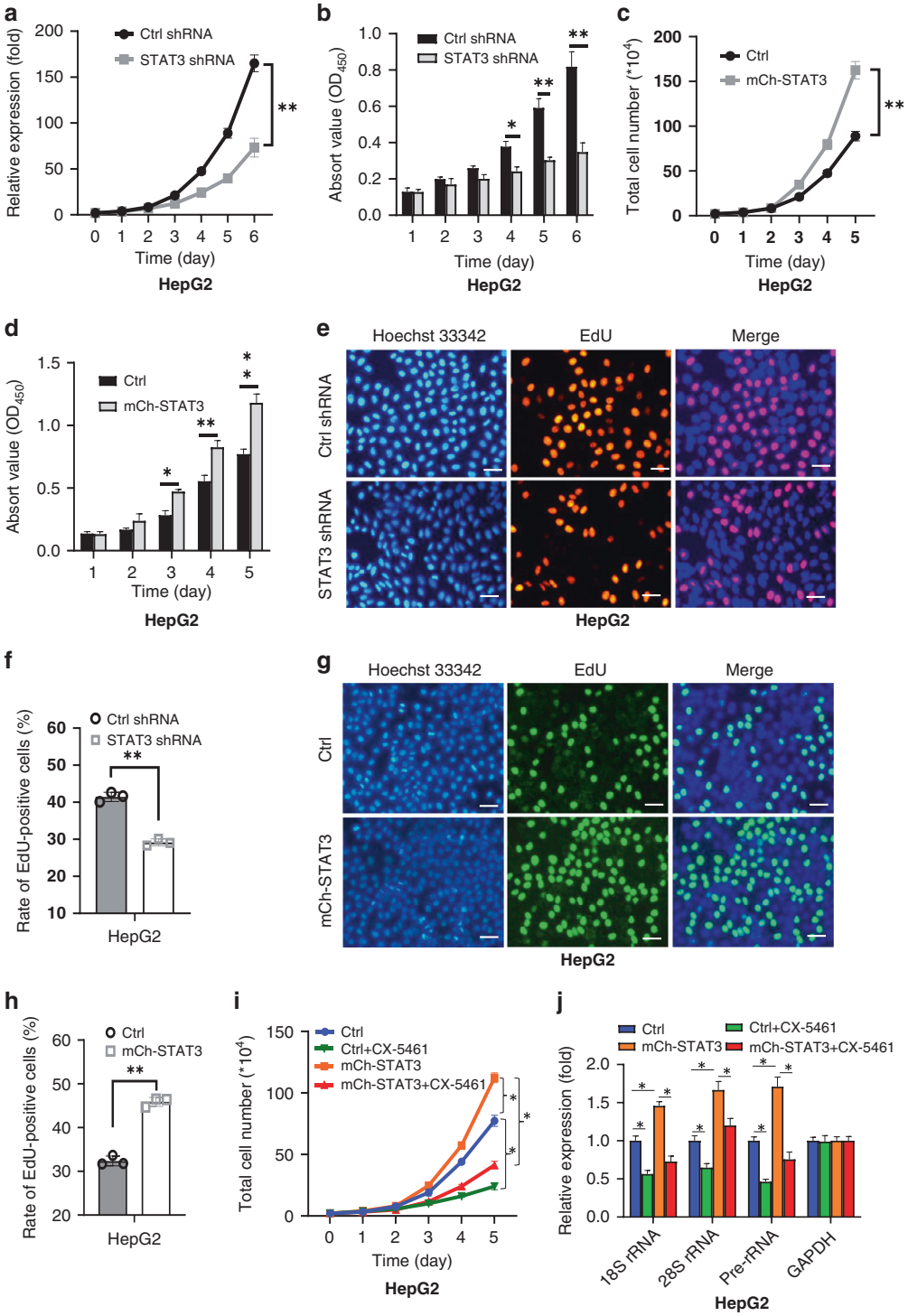

drug (Fig. 5e–g), indicating that the application of two drugs has additive effect on the inhibition of colony formation.

To determine whether these results can be reproduced in vivo, we injected HepG2 cells into nude mice ($n = 6$ for each group) to allow them form tumors for 5 days. The mice bearing a tumor were treated with different combinations of drugs. Analysis of tumor sizes revealed that the average size of the tumors from the mice treated with drugs was significantly smaller than that from the mice treated with 0.9% NaCl. Furthermore, drug treatments did not affect the weights of mice significantly (Fig. 5h, i). Strikingly, the treatments with both of CX-5461 and STAT3-IN-3 exhibited greater inhibition to tumor volumes and weights compared to the treatments with CX-5461 or STAT3-IN-3 only (Fig. 5h, j, k). Collectively, these data indicate that the application of both CX-5461 and STAT3-IN-3 has additive effect on the suppression of HepG2 cell growth in vitro and in vivo compared to the application of CX-5461 or STAT3-IN-3.

Messenger RNA-seq revealed the regulation of RPA34 expression by STAT3

To understand how STAT3 regulates Pol I-directed transcription, we first determined whether STAT3 can be localized to the

Fig. 3 STAT3 promotes cancer cell proliferation. a, **b** STAT3 knockdown reduced HepG2 cell proliferative activity. HepG2 cell lines expressing STAT3 shRNA or control shRNA were used to analyze proliferative activity by cell counting (**a**) and CCK-8 (**b**) methods. **c**, **d** STAT3 overexpression enhanced HepG2 cell proliferative activity. Proliferation assays were performed by cell counting (**c**) and CCK-8 (**d**) methods using a HepG2 cell line stably expressing mCherry-STAT3 and its control cell line. **e** Representative images for EdU assays using HepG2 cell lines stably expressing STAT3 shRNA or control shRNA. EdU specimens were observed and imaged under a fluorescence microscope. The scale bars in images represent 50 μm. **f** Statistical analysis of the EdU-labeled cells based on the EdU assays described in **e**. The rate of EdU positive cells represents the number of EdU-labeled cells in the number of total cells counted in the images. **g** Representative images for EdU assays using a HepG2 cell line expressing mCherry-STAT3 and its control cell line. The scale bars in images represent 50 μm. **h** Statistical analysis of the EdU-labeled cells based on the EdU assays described in **g**. The rate of the EdU positive cells was obtained as for **f**. **i** CX-5461 inhibited the enhancement of HepG2 cell proliferation caused by STAT3 overexpression. Cell proliferation assays were performed using a HepG2 cell line stably expressing mCherry-STAT3 and its control cell line cultured with or without CX-5461 (5 μM). **j** CX-5461 inhibited the activation of Pol I–directed transcription caused by STAT3 overexpression. HepG2 cell lines treated with an inhibitor for 2 days were harvested for the analysis of Pol I products. Each point/column in graphs represents the mean ± SD of three independent experiments ($n = 3$). *$P < 0.05$; **$P < 0.01$. P values in **a**–**d** and **i** were obtained by two-way ANOVA, P values in **f**, **h** and **j** were obtained by Student's t test, performed with control and treatment groups.

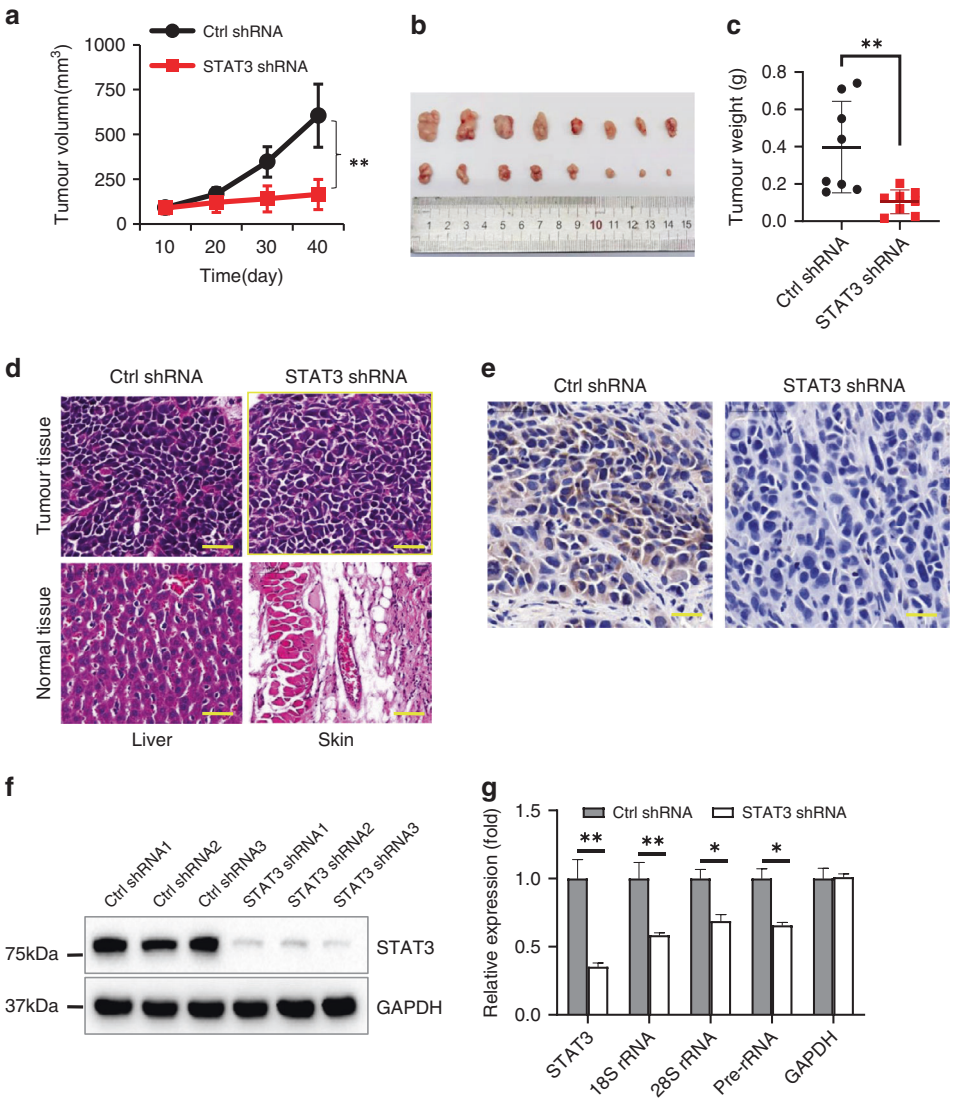

Fig. 4 STAT3 downregulation inhibited tumor cell growth in vivo. a STAT3 knockdown reduced the sizes of tumors formed in nude mice. HepG2 cell lines expressing STAT3 shRNA or control RNA were subcutaneously injected into the back of nude mice ($n = 8$). One week post-injection, tumors formed in mice were measured every 3 days until the mice were euthanized; the resulting data were subjected to statistical analysis. **b** A image showing the effect of STAT3 downregulation on the tumor sizes formed in nude mice. **c** STAT3 downregulation significantly reduced tumor weight. The tumors obtained in B were weighed and subjected to statistical analysis. **d** Comparison of hematoxylin and eosin staining between tumor tissue and the normal tissues as indicated. The tissues from the tumor, liver or skin were fixed, sectioned and used for Hematoxylin and eosin staining. The scale bars in images represent 100 μm. **e** Immunohistochemistry images showing the difference of STAT3 expression between the tissues expressing STAT3 shRNA and control shRNA. **f** Immunoblotting analysis of STAT3 expression in the tissues expressing STAT3 shRNA or control shRNA. **g** Analysis of Pol I products by RT-qPCR in the tissues expressing STAT3 shRNA or control shRNA. Each point/column in histograms represents the mean ± SD of 8 biological replicates ($n = 8$). *$P < 0.05$; **$P < 0.01$. P values obtained by two-way ANOVA (**a**) or Student's t test (**c** and **g**).

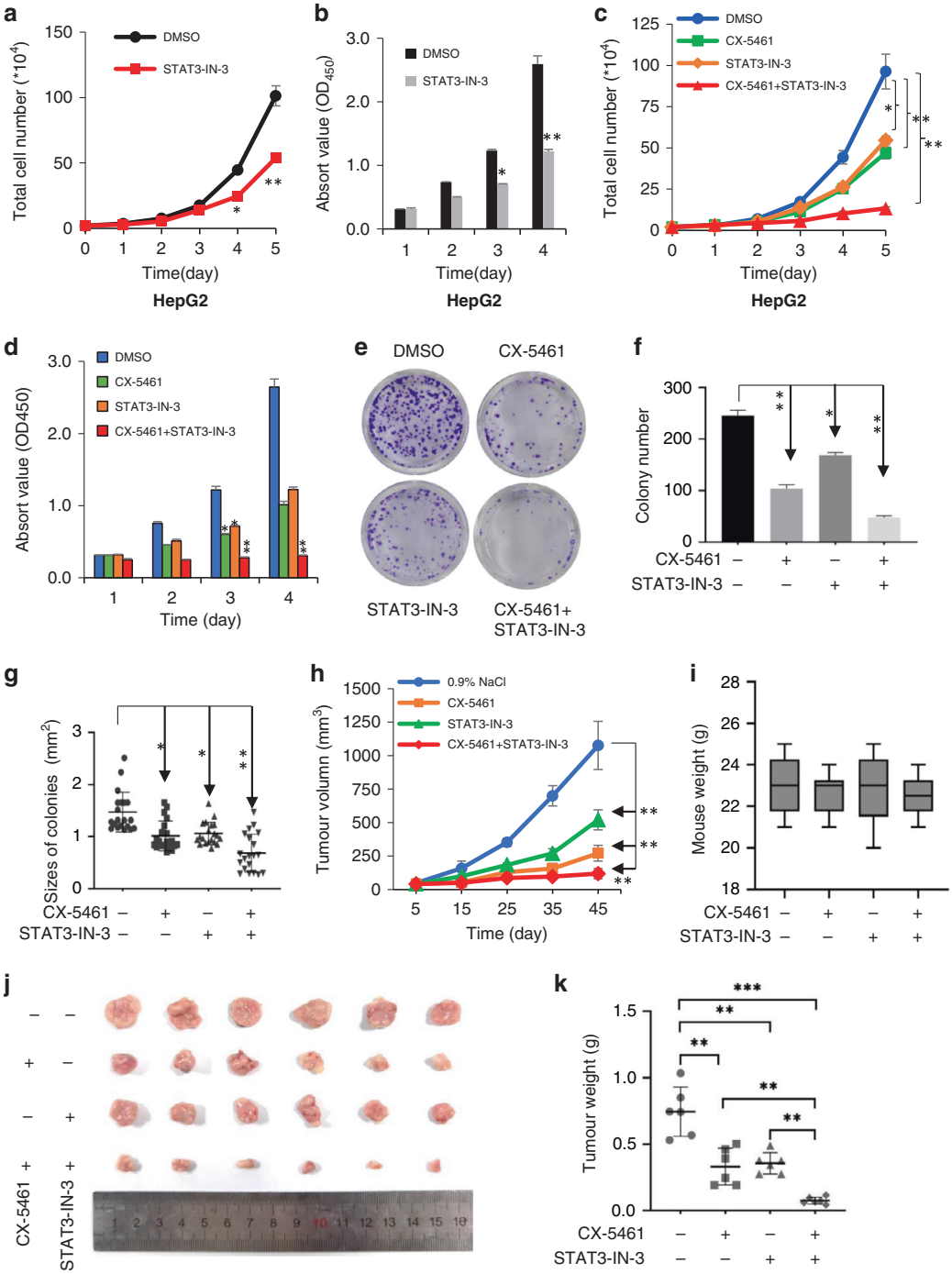

Fig. 5 STAT3-IN-3 and CX-5461 showed an additive effect on the inhibition of tumor cell growth in vitro and in vivo. a, **b** The presence of STAT3-IN-3 decreased HepG2 cell proliferation in vitro. Cell proliferation assays were performed using cell counting (**a**) and CCK-8 (**b**) methods. **c**, **d** Effect of STAT3-IN-3 and CX-5461 on tumor cell growth in vitro. HepG2 cell proliferation was measured with cell counting (**c**) and CCK-8 (**d**) methods. **e**–**g** Effect of STAT3-IN-3 and CX-5461 on the colony formation of HepG2 cells. Colony formation assays were performed using HepG2 cells treated with drugs as indicated. After 10 days, cells were subjected to fixation, staining and imaging (**e**); the number (**f**) and sizes (**g**) of colonies in the images were analyzed statistically. **h** A plot showing the volumes of tumors measured during tumor formation in the mice treated with different drugs. i A graph showing the weights of the mice treated with different drugs after tumors were removed. **j** An image showing the tumors obtained from the mice treated with different drugs. **k** Statistical analysis of the tumors obtained from the mice treated with different drugs. Each point/column in histograms represents the mean ± SD of three independent experiments (**a**–**d**) or 6 biological replicates (**h**, **i** and **k**). *$P < 0.05$; **$P < 0.01$. P values were obtained by two-way ANOVA (**a**–**d** and **h**) or Student's t test (**f**, **g** and **k**).

nucleoli of human cells. Immunofluorescence (IF) assays were performed using HeLa and HepG2 cells and the antibodies against STAT3 or Fibrillarin (a nucleolar protein marker). Unexpectedly, STAT3 couldn't be observed in the nucleoli of these cells (Supplementary Fig. S11), suggesting that STAT3 indirectly regulates Pol I-mediated transcription. To gain a clue about how STAT3 modulates Pol I-directed transcription, we performed RNA-seq analysis using the total RNA extracted from HepG2 cell lines stably expressing STAT3 shRNA or control shRNA. RNA-seq analysis showed that STAT3 silencing caused expression downregulation

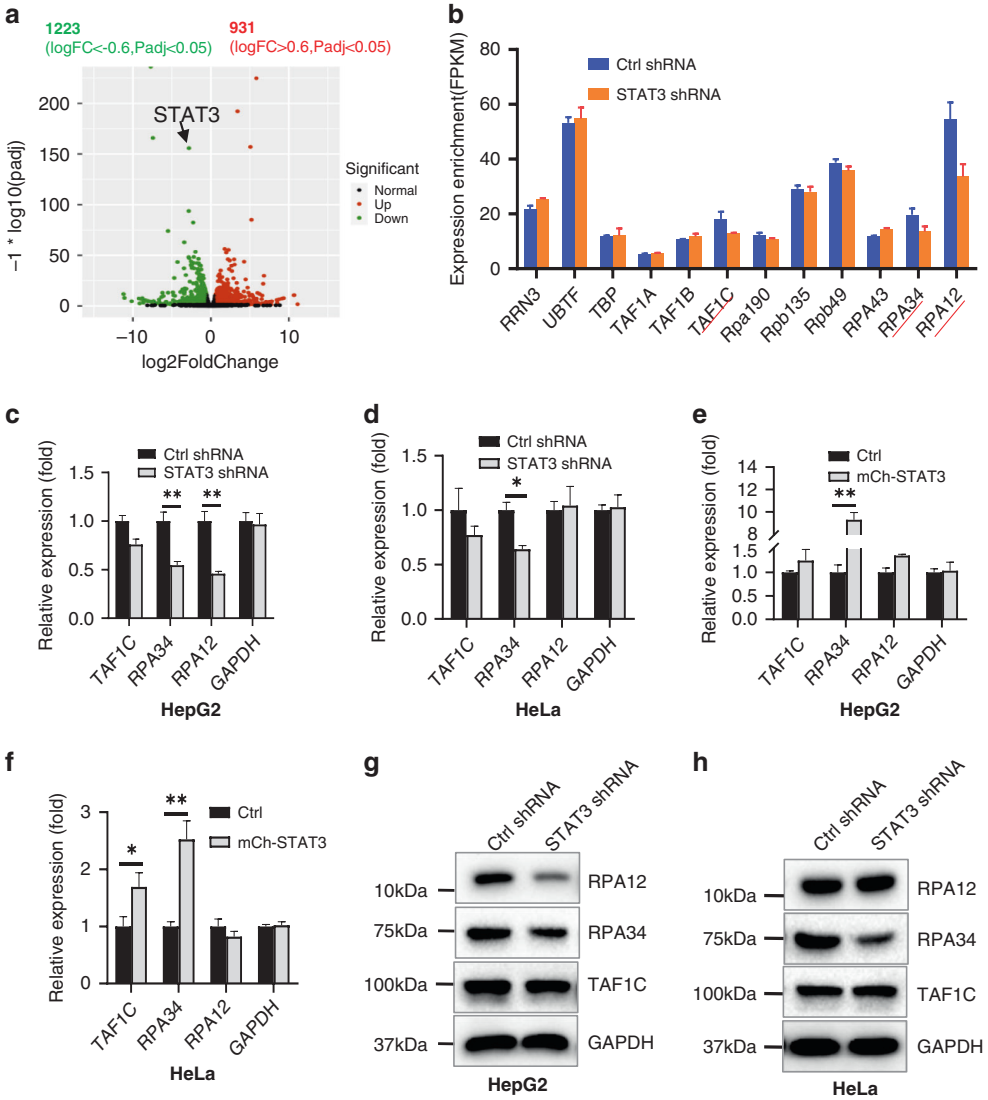

Fig. 6 STAT3 expression positively correlates with RPA34 expression at both RNA and protein levels. a A volcano plot showing the number of upregulated and downregulated differential expression genes (DEGs) based on the mRNA-seq data of HepG2 cell lines expressing STAT3 shRNA or control shRNA. The significant DEGs were defined by the differential expression that is over 1.5-fold between the reads of STAT3 shRNA and control shRNA. **b** Analysis of mRNA expression (FPKM) for the genes encoding Pol I transcription machinery factors. The expression of genes presented in the graph was analyzed from the mRNA dataset detected by mRNA-seq, where differential expression genes were underscored by red lines. **c**, **d** RT-qPCR was used to verify the effect of STAT3 silencing on mRNA expression of RPA12, RPA34 and TAF1C in HepG2 (**c**) and HeLa (**d**) cells. **e**, **f** RT-qPCR was used to analyze the effect of STAT3 overexpression on the expression of RPA12, RPA34 and TAF1C in HepG2 (**e**) and HeLa (**f**) cells. **g**, **h** Western blot results showing the effect of STAT3 knockdown on the expression of RPA12, RPA34 and TAF1C in HepG2 (**g**) and HeLa (**h**) cells. Each point/column in digital graphs represents the mean ± SD of three biological replicates (**a**, **b**) or three independent experiments (**c**–**f**). *$P < 0.05$; **$P < 0.01$. *P* values were obtained by Student's *t* test, performed with control and treatment groups.

of 1223 genes and expression upregulation of 931 genes (Fig. 6a). Analysis of gene ontology (GO) and pathways revealed that significant differential expression genes (DEGs) induced by STAT3 silencing in HepG2 cells contain ribosome-related GO terms or pathways (Supplementary Fig. S12A, B), indicating that STAT3 expression is associated with ribosome pathway. Indeed, Pol I product alteration has been shown to affect ribosome biogenesis [35, 36]. Unexpectedly, among significant DEGs (log_2 fold change > 0.6), the genes encoding any of the Pol I transcription machinery factors couldn't be found. Next, we examined all expression dataset by removing the threshold of significant difference. Consequently, the expression of three genes encoding Pol I machinery factors such as RPA12, RPA34 and TAF1C showed reasonable reduction after STAT3 silencing (Fig. 6b). RT-qPCR confirmed that RPA34 mRNA expression was affected by both STAT3 silencing and overexpression in both HeLa and HepG2 cells, whereas alteration of RPA12 and TAF1C expression showed inconsistency between HeLa and HepG2 cell lines or between STAT3 depletion and overexpression (Fig. 6c–f). Western blotting confirmed that STAT3 silencing reduced RPA34 protein expression in both HepG2 and HeLa cells, whereas TAF1C expression was not affected by STAT3 knockdown in both cell types. Unexpectedly, RPA12 expression was affected by STAT3 silencing in HepG2 cells but not in HeLa cells (Fig. 6g, h). Since RPA34 is usually located in the nucleoli of human cells, we next examined whether alteration of STAT3 expression affects RPA34 levels in the nucleoli by performing immunofluorescence (IF) staining. IF data showed that STAT3 silencing reduced the RPA34 levels in the nucleoli of HepG2

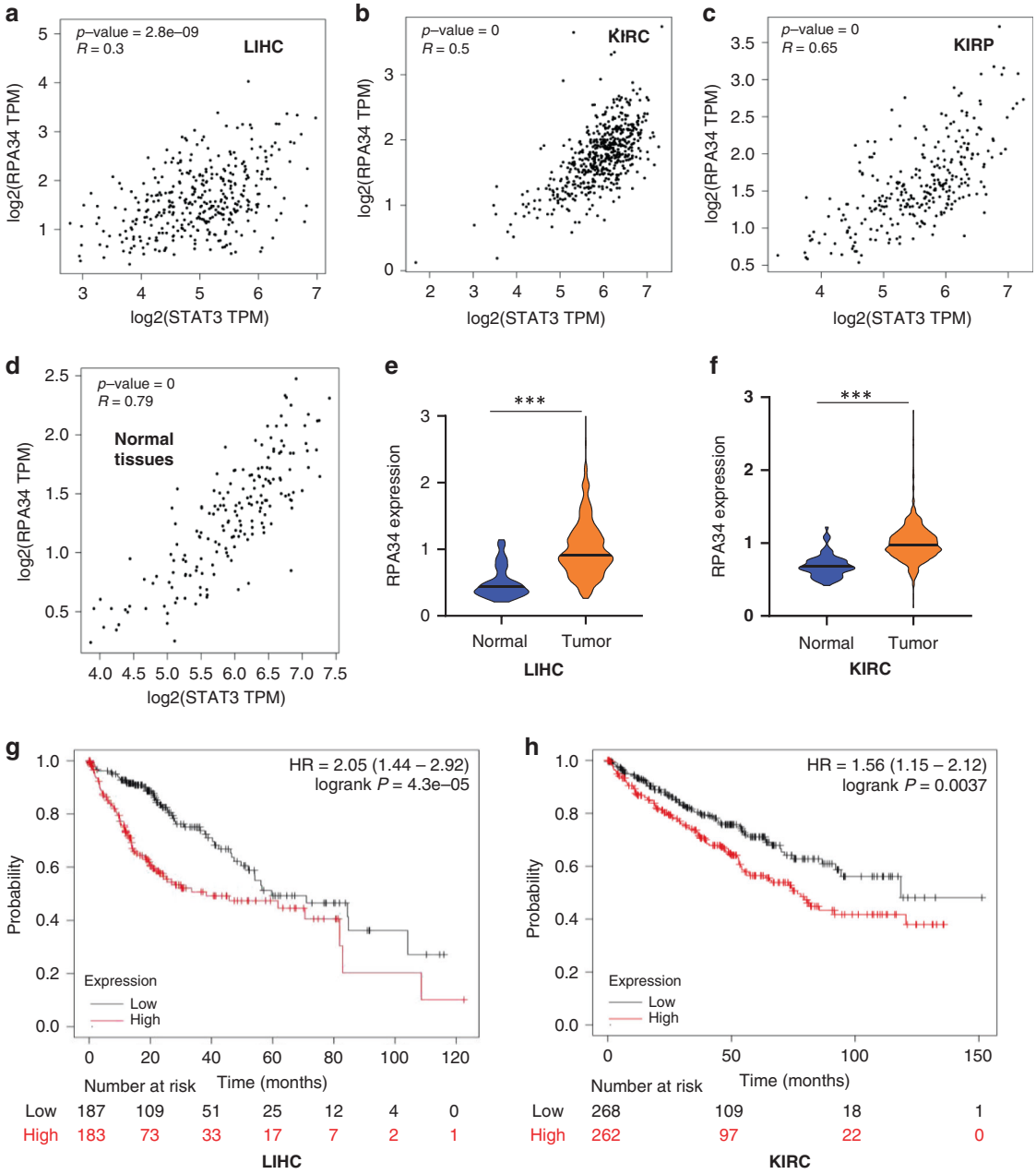

Fig. 7 The relationship between RPA34 expression levels and survival probability and survival time in cancers. a–c Pearson correlation analysis based on the TCGA dataset of clinical cancer samples, including liver hepatocellular carcinoma (LIHC), kidney renal clear cell carcinoma (KIRC) and kidney renal papillary cell carcinoma (KIRP), using the GEPIA online tool (http://gepia2.cancer-pku.cn/#index). **d** Pearson correlation analysis based on the TCGA dataset of normal tissues, including liver, cervix and kidney tissues using the GEPIA online tool (http://gepia2.cancer-pku.cn/#index). **e, f** Violin plots showing RPA34 expression differentiation between normal tissues and liver hepatocellular carcinomas (LIHC) or Kidney renal carcinomas (KIRC). **g, h** Kaplan–Meier Plots showing the relationship between RPA34 expression levels and survival probability and survival time based on the TCGA dataset of liver hepatocellular carcinomas (LIHC) and Kidney renal carcinoma (KIRC). Low: RPA34 low expression, High: RPA34 high expression. High and Low expression levels were determined by the expression median of cancer samples. ***$P < 0.001$, P values were obtained by Student's t test performed by normal and cancer samples (**e**, **f**).

cells compared to the control cell line (Supplementary Fig. S13). Taken together, these results indicate that STAT3 can positively regulate RPA34 expression at both RNA and protein levels in HepG2 and HeLa cells.

Cancer patients with RPA34 abnormal high expression lead to low survival probability

The results obtained above (Fig. 6) suggest a positive regulatory relationship between STAT3 and RPA34. To further confirm this observation, we performed the analysis of Pearson correlation between STAT3 and RPA34 based on the RNA-seq data of cancer samples deposited at The Cancer Genome Atlas (TCGA). Interestingly, positive correlation between STAT3 and RPA34 expression was observed in several cancer types, including liver hepatocellular carcinoma (LIHC, R = 0.3), kidney renal clear cell carcinoma (KIRC, R = 0.5), kidney renal papillary cell carcinoma (KIRP, R = 0.65), thymoma (THYM, R = 0.77), diffuse large B-cell lymphoma (DLBC, R = 0.69) and thyroid carcinoma (THCA, R = 0.63) (Fig. 7a–c, Supplementary Fig. S14). Further, strong positive correlation (R = 0.79) between STAT3 and RPA34 expression was

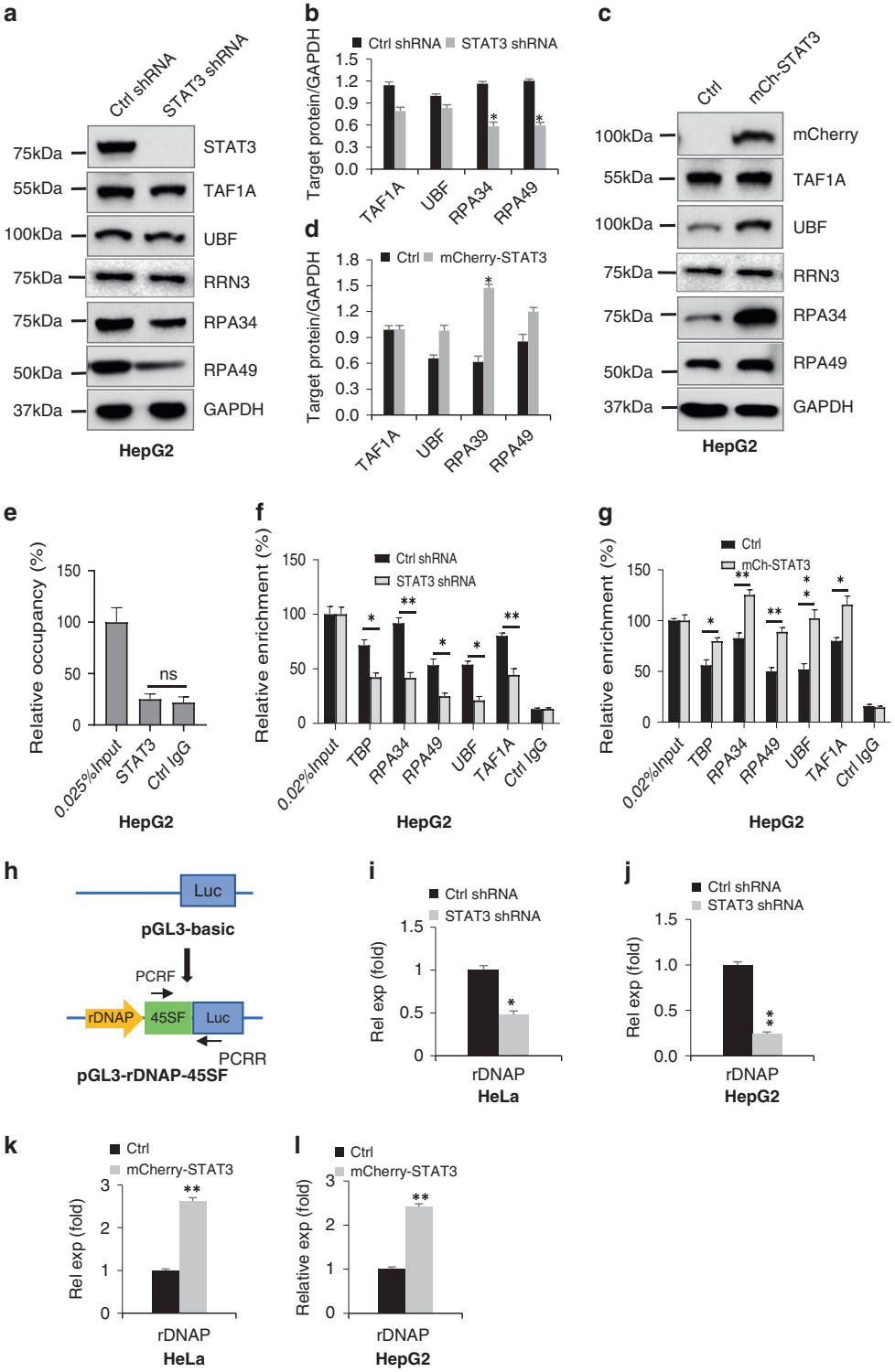

also observed in normal tissues when Pearson correlation analysis was performed using the RNA-seq data of liver, cervix and kidney tissues deposited at the TCGA (Fig. 7d). Next, we analyzed the expression difference of RPA34 between cancer cells and normal cells by Western blot. Clearly, both HeLa and HepG2 cells have higher RPA34 expression than their normal cell lines, HUCEC and HL-7702, respectively (Supplementary Fig. S15A, B). Interestingly, the presence of STAT3-IN-3 dampened RPA34 expression in both HeLa and HepG2 cells (Supplementary Fig. S15C, D). We next determined whether the expression difference of RPA34 between cancer and normal tissues is similar to that between tumor and normal cell lines. Thus, RPA34 expression was analyzed based on the RNA-seq data in the TCGA database, and the results were presented in Fig. 7e, f. Apparently, both liver hepatocellular carcinomas (LIHC) and kidney renal carcinomas (KIRC) showed higher RPA34 expression than their normal tissues. We then addressed whether high levels of RPA34 expression can affect cancer patient survival rate. To this end, we performed

Fig. 8 STAT3 regulates the assembly of components of the Pol I transcription machinery at the rDNA promoter by affecting RPA34 expression. a, **b** Effect of STAT3 knockdown on the expression of the Pol I-related factors was analyzed by Western blot using HepG2 cells expressing STAT3 shRNA or control shRNA and antibodies as indicated (**a**). The quantified result of Western blots ($n = 3$) is shown in **b**. **c**, **d** Effect of STAT3 overexpression on the expression of Pol I-related factors by Western blot using HepG2 cells with STAT3 overexpression. **d** represents the quantified result of Western blots in **c** ($n = 3$). **e** STAT3 does not bind to the rDNA promoter. HepG2 cells were used for ChIP assays using an anti-STAT3 antibody, where the DNA recovered from the chromatin immunoprecipitation was analyzed by qPCR. Relative enrichment was obtained by comparing the relative quantity of target DNA in 1 μL of ChIP samples to that from 0.025% input. **f** STAT3 downregulation reduced the occupancies of the Pol I transcription machinery factors at the rDNA promoter. ChIP assays were performed using HepG2 cell lines expressing STAT3 shRNA or control shRNA and antibodies against the factors as indicated. **g** STAT3 upregulation increased the occupancies of the Pol I transcription machinery factors at the rDNA promoter. ChIP assays were performed using a HepG2 cell line expressing mCherry-STAT3 and its control cell line in which antibodies against factors used for the assays were as indicated. **h** A scheme showing the cloning of the rDNA promoter (rDNAP) with the reporter vector pGL3-basic. 45SF: 45S DNA fragment; Luc: luciferase. **i**, **j** STAT3 knockdown inhibited the rDNA promoter activity. The "reporter" gene expression was detected by RT-qPCR using the primers as indicated in **h** after transfection of the rDNA promoter (rDNAP)-driving reporter vectors into HeLa (**i**) or HepG2 (**j**) cell lines. Rel exp: relative expression. **k**, **l** STAT3 overexpression inhibited the rDNA promoter activity. The "reporter" gene expression was monitored by RT-qPCR after transfecting the rDNA promoter-driving reporter vectors into HeLa (**k**) and HepG2 (**l**) cell lines. Each column in histograms represents the mean ± SD of three independent experiments. $^{*}P < 0.05$; $^{**}P < 0.01$. *P* values were obtained by Student's *t* test.

Kaplan–Meier plotting using the RNA-seq dataset of liver hepatocellular carcinomas (LIHC) and kidney renal carcinoma (KIRC) obtained from the TCGA database. We showed that the patients with RPA34 high expression levels in liver hepatocellular carcinomas (LIHC) or kidney renal carcinomas (KIRC) exhibited lower survival probability and shorter survival time when compared to the patients with low RPA34 expression levels. Taken together, cancer patients with high levels of RPA34 expression may lead to low survival rate, suggesting that RPA34 may act as a biomarker of poor prognosis in a subset of cancers.

STAT3 modulates the recruitment of the Pol I transcription machinery components to the rDNA promoter by controlling RPA34 expression

Apart from RPA34, whether alteration of STAT3 expression affects the expression of other factors related to Pol I transcription at the protein level is unclear. Thus, we analyzed the expression of a few factors related to Pol I transcription apparatus by Western blot using cell lines with STAT3 silencing or overexpression. Immunoblotting results showed that both STAT3 upregulation and downregulation affected RPA34 expression in HeLa and HepG2 cells. However, the expression of UBF, TAF1A, and RPA49 was variable between two cell types or between STAT3 knockdown and overexpression samples (Fig. 8a–d, Supplementary Fig. S16). Since STAT3 positively regulates the synthesis of Pol I products, we determined whether STAT3 binds to the rDNA promoter by performing ChIP assays. ChIP qPCR data showed that STAT3 does not bind to the rDNA promoter (Fig. 8e). This result is consistent with that obtained in IF assays (Supplementary Fig. S11). We next investigated whether alteration of STAT3 expression affects the assembly of the Pol I transcription machinery factors at the rDNA promoter by performing ChIP assays using HepG2 cells. We showed that STAT3 silencing reduced the occupancies of the Pol I transcription machinery factors at the rDNA promoter, while STAT3 overexpression enhanced the occupancies of these factors at the promoter (Fig. 8f, g), suggesting that STAT3 can modulate the recruitment of the Pol I transcription machinery factors to the rDNA promoter by affecting RPA34 expression. Next, we addressed whether alteration of STAT3 expression can affect the rDNA promoter (rDNAP) activity. To achieve this goal, we amplified the rDNA promoter along with the DNA fragment encoding about 300 nt 45S pre-rRNA immediately downstream of the promoter, the resulting DNA was inserted into the pGL3-basic. The promoter-driven reporter vectors were transfected into HeLa and HepG2 cell lines. RT-qPCR was used to detect the expression of a 'reporter' gene using the primers as indicated in Fig. 8h. The results showed that STAT3 knockdown inhibited the rDNAP activity; whereas STAT3 overexpression activated the rDNAP activity in both of cell types (Fig. 8i–l). Collectively, these data indicate that STAT3 can modulate the recruitment of components of the Pol I transcription machinery to the rDNA promoter by controlling RPA34 expression, which consequently affects the transcription activity of the rDNA promoter.

STAT3 regulates *Rpa34* gene transcription by binding to the *Rpa34* promoter

To determine whether RPA34 is required for the regulation of Pol I transcription mediated by STAT3, we performed rescue experiments by expressing mCherry-RPA34 in HepG2 and HeLa cell lines with STAT3 depletion. The results from the rescue experiments showed that mCherry-RPA34 expression reversed the inhibition of Pol I-directed transcription induced by the STAT3 silencing (Fig. 9a, b, Supplementary Fig. S17A, B) and alleviate the repression of HepG2 cell growth caused by STAT3 silencing (Fig. 9c, d, Supplementary Fig. S17C, D), indicating that RPA34 participates in the regulation of Pol I-directed transcription mediated by STAT3. We then determined whether RPA34 expression alteration affects the synthesis of Pol I products by in HepG2 and HeLa cells using a lentiviral expression system. We showed that RPA34 silencing reduced the synthesis of Pol I products (Fig. 9e, f, Supplementary Fig. S17E, F). In contrast, RPA34 overexpression increased Pol I product expression (Fig. 9g, h, Supplementary Fig. S17G, H), indicating RPA34 positively regulates the synthesis of Pol I products. To understand how STAT3 regulates RPA34 expression, we searched for the STAT3-binding motif in the *Rpa34* gene promoter. Surprisingly, the *Rpa34* promoter contains two putative STAT3 consensus sequences upstream of the transcription start site (Fig. 9i). ChIP assays confirmed that STAT3 can bind to the *Rpa34* promoter (Fig. 9j). Next, the *Rpa34* promoter was inserted into the pGL3-basic reporter vector and the *Rpa34* promoter activity was examined by performing luciferase assays. We showed that STAT3 silencing reduced the *Rpa34* promoter activity, while STAT3 overexpression enhanced its activity (Fig. 9k, l, Supplementary Fig. S17I, J). Mutations of STAT3 binding sites blunted the activity of the *Rpa34* promoter (Fig. 9m, n), indicating that STAT3 controls *Rpa34* gene expression at the transcription step. To further understand how STAT3 regulates *Rpa34* gene transcription, we performed ChIP assays using HepG2 cell lines expressing STAT3 shRNA or control shRNA. ChIP-qPCR showed that STAT3 silencing inhibited the assembly of the RNA polymerase II transcription machinery factors at the *Rpa34* promoter (Fig. 9o). These data suggest that STAT3 regulates *Rpa34* gene transcription by affecting the recruitment of Pol II transcription machinery factors to the *Rpa34* promoter.

Based on the data obtained in this study, we proposed a model by which STAT3 regulates Pol I-directed transcription. Specifically, after phosphorylation, STAT3 enters nuclei and directly binds to the *Rpa34* promoter to modulate *Rpa34* gene transcription. After

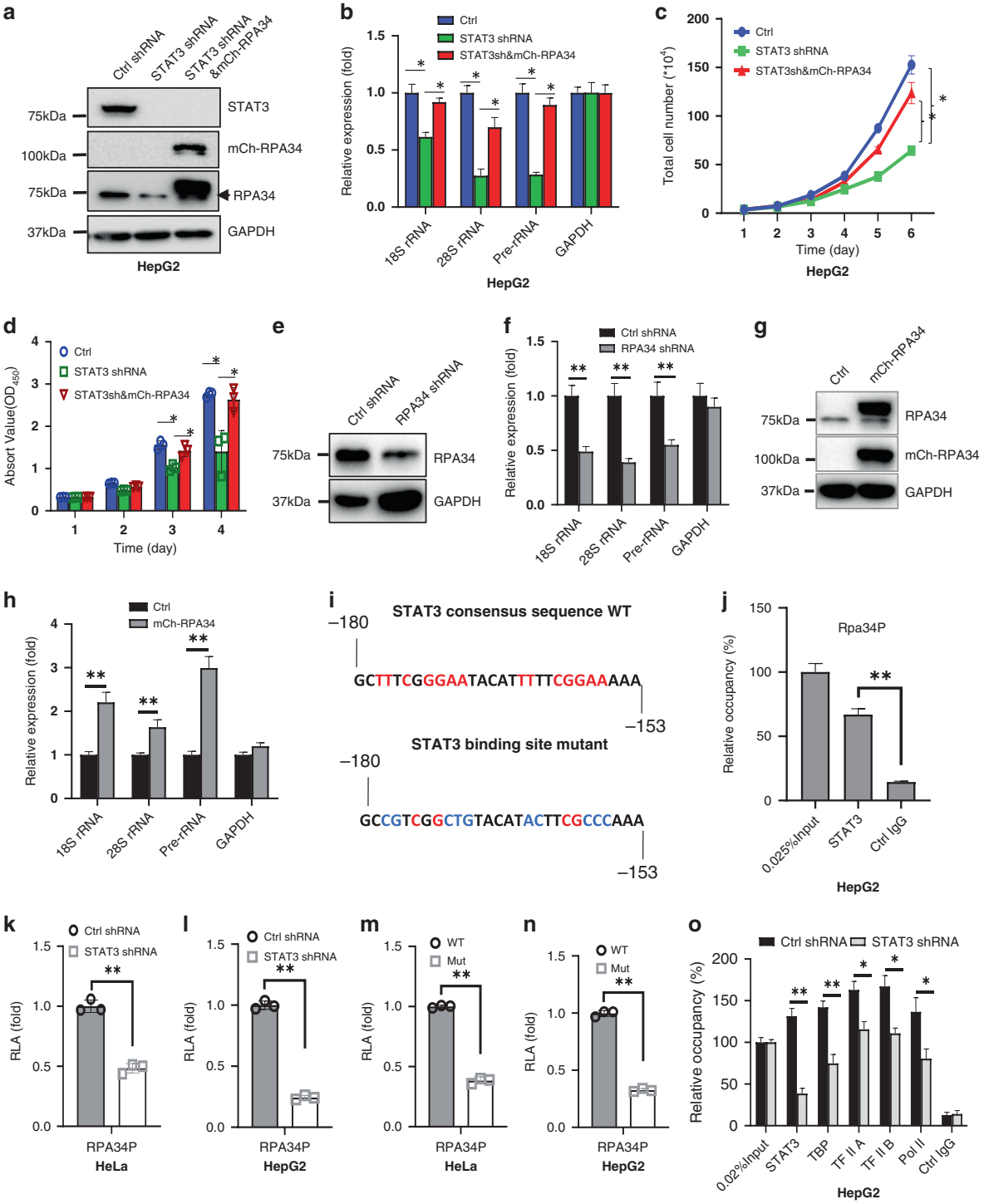

translation in cytoplasm, RPA34 enters the nucleoli of human cells and binds to the rDNA promoter along with other factors of the Pol I transcription machinery. Consequently, STAT3 modulates Pol I-directed transcription by controlling RPA34 expression and the assembly of the Pol I transcription machinery at the rDNA promoter (Fig. 10).

DISCUSSION

Previous studies showed that STAT3 can be activated by canonical signaling pathways. Upon activation, STAT3 is phosphorylated and forms a homodimer to enter the nucleus, where phosphorylated STAT3 regulates the transcription of target genes directed by RNA polymerase II [1, 2]. In this study, however, we found that STAT3 can positively regulate 45S ribosomal RNA expression. Thus, we identified a novel role of STAT3 in transcriptional regulation in this work. This finding seems contradiction with the initial observation in FLNA-depleted SaOS2 cells, where FLNA silencing reduced STAT3 expression (Supplementary Fig. S1) but increased expression of Pol I products [44]. This discrepancy may be because thousands of differential expression genes were downregulation and upregulation in FLNA-depleted SaOS2 cells [50], and STAT3

Fig. 9 STAT3 modulates Pol I–directed transcription by controlling RPA34 transcription. a Generation of HepG2 cell lines stably expressing both STAT3 shRNA and mCherry-RPA34. Western blot was used to verify HepG2 cell lines expressing STAT3 shRNA only or both STAT3 and mCherry-STAT3 and the control cell line using antibodies as indicated. **b** Analysis of Pol I products by RT-qPCR using the cell lines established in **a**. **c**, **d** Cell proliferation assays for the cell lines established in **a**. Cell proliferation assays were performed using cell counting (**c**) and CCK-8 (**d**) methods. **e**, **f** Effect of RPA34 silencing on Pol I-directed transcription in HepG2 cells. RPA34 and Pol I products were analyzed by Western blot (**e**) and RT-qPCR (**f**), respectively. **g**, **h** Effect of RPA34 overexpression on Pol I-directed transcription in HepG2 cells. RPA34 and Pol I products were analyzed by Western blot (**g**) and RT-qPCR (**h**), respectively. **i** A cartoon showing putative STAT3 binding elements in the *Rpa34* promoter. Red letters represent STAT3 consensus bases (WT), while blue letters represent the mutations of STAT3 consensus bases. **j** A ChIP result showing the STAT3 occupancy at the *Rpa34* promoter in HepG2 cells. **k**, **l** STAT3 inhibited the *Rpa34* promoter activity in HeLa and HepG2 cells. Luciferase assays were performed by transfecting the RPA34P-driving reporter vectors into HeLa and HepG2 cell lines expressing STAT3 shRNA or control shRNA. Relative luciferase activity (RLA) was obtained by comparing the luciferase activity of treatment samples to that of control samples, where the activity of control samples was arbitrarily set as 1. **m**, **n** Mutations of the STAT3 consensus bases suppressed the *Rpa34* promoter activity. The reporter vectors driven by the wild type RPA34P or by its mutant containing STAT3-binding site mutations were transfected into HeLa and HepG2 cells. RLA, relative luciferase activity. **o** STAT3 downregulation inhibited the occupancies of the Pol II transcription machinery factors at the *Rpa34* promoter. ChIP assays were performed using HepG2 cell lines expressing STAT3 shRNA or control shRNA and the antibodies against the factors as indicated. The relative occupancy was obtained as described in Fig. 6a. Each column in the histograms represents the mean ± SD of three independent experiments. $*P < 0.05$; $**P < 0.01$. *P* values were obtained by two-way ANOVA (**b**–**d**) or Student's *t* test (**f**, **h**, **j**–**o**).

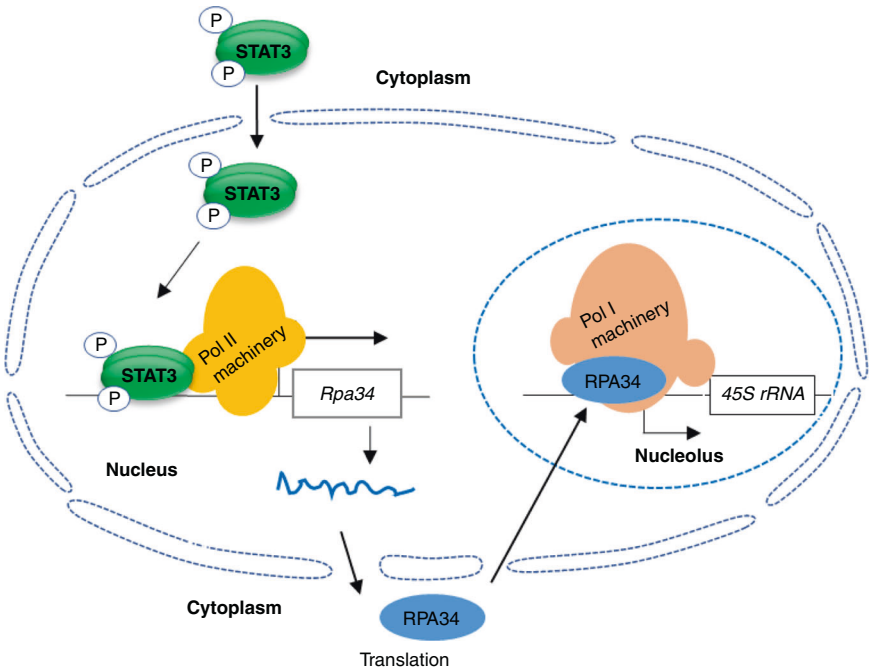

Fig. 10 A proposed model by which STAT3 modulates Pol I-directed transcription. After phosphorylation, p-STAT3 enters nuclei and binds to the *Rpa34* promoter to transcribe RPA34 mRNA. After translation, RPA34 protein enters nucleoli and binds to the rDNA promoter to initiate Pol I-directed transcription.

might not play a key role in this situation; instead, FLNA acts as a key regulator in Pol I-directed transcription and regulates it by a sequestration mode [44]. In recent years, many novel factors, including non-coding RNA and proteins, have been shown to regulate cancer development by affecting STAT3 signaling [3, 25, 51, 52]. Thus, the function of STAT3 identified in this study extends the understanding of the regulatory mechanism of gene transcription and cancer development mediated by STAT3. We showed that STAT3 can activate RPA34 expression but not expression of Pol I general transcription factors (Figs. 6 and 8), and STAT3 enhances the recruitment of the Pol I transcription machinery to the rDNA promoter by increasing RPA34 expression (Fig. 8). Furthermore, STAT3 activates *Rpa34* gene transcription by binding to the *Rpa34* promoter, and RPA34 silencing affected the synthesis of Pol I products [Fig. 9], indicating that STAT3 regulates Pol I-dependent transcription by controlling RPA34 expression, This result is distinct from the previous findings in which the oncogenic factor MYC regulates Pol I-dependent transcription by interacting with the ribosomal DNA promoter rather than Pol I subunit [39, 53]. This study provides a novel mechanism by which the oncogenic factor STAT3 modulate Pol I-dependent transcription

STAT3 has become an appealing target for anti-cancer therapy due to its activating role in cancer development for a subset of cancers [1, 3]. In this work, we found that STAT3 has higher expression in HeLa and HepG2 cells than it does in normal cells, and STAT3 promotes proliferation activity for these cell types. Additionally, abnormal high expression of its downstream factor RPA34 in a subset of cancers was observed, and cancer patients with high expression of RPA34 have lower survival rate and shorter survival time compared those with low expression of RPA34 (Fig. 7). These data suggest that STAT3 may modulate cancer development by influencing the expression of its downstream factor RPA34, and RPA34 can act as a biomarker of poor prognosis in subset of cancer types. Intriguingly, the presence of STAT3-IN-3 can severely inhibit cell proliferation and induce cell

death (Figs. 2, 3 and 5; Supplementary Figs. S4–8, and S10). Additionally, the Pol I-specific inhibitor CX5461 represses proliferation activity for these cell types by inhibiting the increase of Pol I products induced by STAT3 overexpression (Fig. 3I, J). These results suggest that tumor cell growth can be concurrently inhibited by STAT3-IN-3 and CX-5461. Indeed, the tumor cells treated with both STAT3-IN-3 and CX-5461 (or BMH-21/Actinomycin D) led to additive effect on cancer cell deaths or cell growth suppression in vitro and in vivo when compared to the cells were treated with either of the inhibitors (Fig. 5, Supplementary Fig. S10A–D). Currently, multiple drugs are often used for anti-cancer research as well as cancer therapy in the clinic [54, 55]. Thus, the result of inhibitor assays has profound medical significance because STAT3-IN-3 and Pol I transcription inhibitors would act as combined drugs in cancer therapy in the future.

CONCLUSIONS

In this study, we identified a positive role of STAT3 in Pol I-directed transcription in human tumor cells. STAT3 positively regulates cancer cell survival and growth in vitro and in vivo. The presence of both of STAT3 and Pol I transcription inhibitors has a greater inhibitory effect on tumor cell growth than the application of either inhibitors. STAT3 activates Rpa34 transcription by binding to the *Rpa34* promoter, which consequently controls Pol I-directed transcription by affecting the Pol I transcription machinery assembly at the rDNA promoter. RPA34 has abnormal high expression in subset of cancer types, and cancer patients with RPA34 high expression exhibits poor prognosis. Our findings provide a novel insight into Pol I–directed transcription and a promising prospect that STAT3 and Pol I-specific inhibitors may act as combined drugs in cancer therapy.

DATA AVAILABILITY

The RNA-seq data about SaOS2 cell FLNA silencing were deposited in the NCBI repository (SRA: SRP318361, https://www.ncbi.nlm.nih.gov/Traces/study/?acc=PRJNA726417). The RNA-seq data about HepG2 cell STAT3 silencing were deposited in the NCBI Gene Expression Omnibus (GSE201548). The RNA-seq data used for Pearson correlation analysis, Kaplan–Meier plotting and Violin plotting were obtained from the TCGA database (www.tcgaportal.org).

REFERENCES

1. Lee H, Jeong AJ, Ye SK. Highlighted STAT3 as a potential drug target for cancer therapy. BMB Rep. 2019;52:415–23.
2. Srivastava J, DiGiovanni J. Non-canonical Stat3 signaling in cancer. Mol Carcinog. 2016;55:1889–98.
3. Yang L, Lin S, Xu L, Lin J, Zhao C, Huang X. Novel activators and small-molecule inhibitors of STAT3 in cancer. Cytokine Growth Factor Rev. 2019;49:10–22.
4. Johnson DE, O'Keefe RA, Grandis JR. Targeting the IL-6/JAK/STAT3 signaling axis in cancer. Nat Rev Clin Oncol. 2018;15:234–48.
5. Chua CY, Liu Y, Granberg KJ, Hu L, Haapasalo H, Annala MJ, et al. IGFBP2 potentiates nuclear EGFR-STAT3 signaling. Oncogene. 2016;35:738–47.
6. Bromberg JF, Wrzeszczynska MH, Devgan G, Zhao Y, Pestell RG, Albanese C, et al. Stat3 as an oncogene. Cell. 1999;98:295–303.
7. Aryappalli P, Shabbiri K, Masad RJ, Al-Marri RH, Haneefa SM, Mohamed YA, et al. Inhibition of tyrosine-phosphorylated STAT3 in human breast and lung cancer cells by manuka honey is mediated by selective antagonism of the IL-6 receptor. Int J Mol Sci. 2019;20:4340.
8. Zhang Q, Raje V, Yakovlev VA, Yacoub A, Szczepanek K, Meier J, et al. Stat3 promotes breast cancer growth via phosphorylation of serine 727. J Biol Chem. 2013;288:31280–8.
9. Wegrzyn J, Potla R, Chwae YJ, Sepuri NB, Zhang Q, Koeck T, et al. Function of mitochondrial Stat3 in cellular respiration. Science. 2009;323:793–7.
10. Gough DJ, Corlett A, Schlessinger K, Wegrzyn J, Larner AC, Levy DE. Mitochondrial STAT3 supports Ras-dependent oncogenic transformation. Science. 2009;324:1713–6.
11. Macias E, Rao D, Carbajal S, Kiguchi K, Digiovanni J. Stat3 binds to mtDNA and regulates mitochondrial gene expression in keratinocytes. J Invest Dermatol. 2014;134:1971–80.
12. Tammineni P, Anugula C, Mohammed F, Anjaneyulu M, Larner AC, Sepuri NB. The import of the transcription factor STAT3 into mitochondria depends on GRIM-19, a component of the electron transport chain. J Biol Chem. 2013;288:4723–32.
13. Braunstein J, Brutsaert S, Olson R, Schindler C. STATs dimerize in the absence of phosphorylation. J Biol Chem. 2003;278:34133–40.
14. Yang JB, Stark GR. Roles of unphosphorylated STATs in signaling. Cell Res. 2008;18:443–51.
15. Yang J, Liao X, Agarwal MK, Barnes L, Auron PE, Stark GR. Unphosphorylated STAT3 accumulates in response to IL-6 and activates transcription by binding to NFkappaB. Genes Dev. 2007;21:1396–408.
16. Yang J, Chatterjee-Kishore M, Staugaitis SM, Nguyen H, Schlessinger K, Levy DE, et al. Novel roles of unphosphorylated STAT3 in oncogenesis and transcriptional regulation. Cancer Res. 2005;65:939–47.
17. Zhao J, Du P, Cui P, Qin Y, Hu C, Wu J, et al. LncRNA PVT1 promotes angiogenesis via activating the STAT3/VEGFA axis in gastric cancer. Oncogene. 2018;37:4094–109.
18. Huang Z, Zhou W, Li Y, Cao M, Wang T, Ma Y, et al. Novel hybrid molecule overcomes the limited response of solid tumors to HDAC inhibitors via suppressing JAK1-STAT3-BCL2 signalling. Theranostics. 2018;8:4995–5011.
19. Su K, Zhao Q, Bian A, Wang C, Cai Y, Zhang Y. A novel positive feedback regulation between long noncoding RNA UICC and IL-6/STAT3 signaling promotes cervical cancer progression. Am J Cancer Res. 2018;8:1176–89.
20. Dai W, Liu S, Zhang J, Pei M, Xiao Y, Li J, et al. Vorinostat triggers miR-769-5p/3p-mediated suppression of proliferation and induces apoptosis via the STAT3-IGF1R-HDAC3 complex in human gastric cancer. Cancer Lett. 2021;S0304-3835:00437–7.
21. Chuang CH, Greenside PG, Rogers ZN, Brady JJ, Yang D, Ma RK, et al. Molecular definition of a metastatic lung cancer state reveals a targetable CD109- Janus kinase-Stat axis. Nat Med. 2017;23:291–300.
22. Jia L, Wang Y, Wang CY. circFAT1 promotes cancer stemness and immune evasion by promoting STAT3 activation. Adv Sci. 2021;8:2003376.
23. Cayrol F, Praditsuktavorn P, Fernando TM, Kwiatkowski N, Marullo R, Calvo-Vidal MN, et al. THZ1 targeting CDK7 suppresses STAT transcriptional activity and sensitizes T-cell lymphomas to BCL2 inhibitors. Nat Commun. 2017;8:14290.
24. He L, Pratt H, Gao M, Wei F, Weng Z, Struhl K. YAP and TAZ are transcriptional coactivators of AP-1 proteins and STAT3 during breast cellular transformation. Elife. 2021;10:e67312.
25. Lv D, Li Y, Zhang W, Alvarez AA, Song L, Tang J, et al. TRIM24 is an oncogenic transcriptional co-activator of STAT3 in glioblastoma. Nat Commun. 2017;8:1454.
26. Wang ST, Ho HJ, Lin JT, Shieh JJ, Wu CY. Simvastatin-induced cell cycle arrest through inhibition of STAT3/SKP2 axis and activation of AMPK to promote p27 and p21 accumulation in hepatocellular carcinoma cells. Cell Death Dis. 2017;8:e2626.
27. Chung SS, Adekoya D, Enenmoh I, Clarke O, Wang P, Sarkyssian M, et al. Salinomycin abolished STAT3 and STAT1 interactions and reduced telomerase activity in colorectal cancer cells. Anticancer Res. 2017;37:445–53.
28. Ahn KS, Sethi G, Sung B, Goel A, Ralhan R, Aggarwal BB. Guggulsterone, a farnesoid X receptor antagonist, inhibits constitutive and inducible STAT3 activation through induction of a protein tyrosine phosphatase SHP-1. Cancer Res. 2008;68:4406–15.
29. Song JM, Qian X, Upadhyayya P, Hong KH, Kassie F. Dimethylaminoparthenolide, a water soluble parthenolide, suppresses lung tumorigenesis through down-regulating the STAT3 signaling pathway. Curr Cancer Drug Targets. 2014;14:59–69.
30. Bai L, Zhou H, Xu R, Zhao Y, Chinnaswamy K, McEachern D, et al. A potent and selective small-molecule degrader of STAT3 achieves complete tumor regression in vivo. Cancer Cell. 2019;36:498–511.
31. Cai G, Yu W, Song D, Zhang W, Guo J, Zhu J, et al. Discovery of fluorescent coumarin-benzo thiophene 1, 1-dioxide conjugates as mitochondria-targeting antitumor STAT3 inhibitors. Eur J Med Chem. 2019;174:236–51.
32. Zhang N, Zhang M, Wang Z, Gao W, Sun ZG. Activated STAT3 could reduce survival in patients with esophageal squamous cell carcinoma by up-regulating VEGF and cyclin D1 expression. J Cancer. 2020;11:1859–68.
33. Bowman T, Broome MA, Sinibaldi D, Wharton W, Pledger WJ, Sedivy JM, et al. Stat3-mediated Myc expression is required for Src transformation and PDGF-induced mitogenesis. Proc Natl Acad Sci USA. 2001;98:7319–24.
34. Gritsko T, Williams A, Turkson J, Kaneko S, Bowman T, Huang M, et al. Persistent activation of stat3 signaling induces survivin gene expression and confers resistance to apoptosis in human breast cancer cells. Clin Cancer Res. 2006;12:11–9.
35. Drygin D, Rice WG, Grummt I. The RNA polymerase I transcription machinery: an emerging target for the treatment of cancer. Annu Rev Pharm Toxicol. 2010;50:131–56.
36. Sharifi S, Bierhoff H. Regulation of RNA polymerase I transcription in development, disease, and aging. Annu Rev Biochem. 2018;87:1–73.

37. Ferreira R, Schneekloth JS Jr, Panov KI, Hannan KM, Hannan RD. Targeting the RNA polymerase I transcription for cancer therapy comes of age. Cells. 2020;9:266.
38. Goodfellow SJ, Zomerdijk JC. Basic mechanism in RNA polymerase I transcription of ribosomal RNA genes. Subcell Biochem. 2013;61:211–36.
39. Arabi A, Wu S, Ridderstråle K, Bierhoff H, Shiue C, Fatyol K, et al. c-Myc associates with ribosomal DNA and activates RNA polymerase I transcription. Nat Cell Biol. 2005;7:303–10.
40. Bywater MJ, Poortinga G, Sanij E, Hein N, Peck A, Cullinane C, et al. Inhibition of RNA polymerase I as a therapeutic strategy to promote cancer-specific activation of p53. Cancer Cell. 2012;22:51–65.
41. Mayer C, Bierhoff H, Grummt I. The nucleolus as a stress sensor: JNK2 inactivates the transcription factor TIF-IA and down-regulates rRNA synthesis. Genes Dev. 2005;19:933–41. Apr 15
42. Tessarz P, Santos-Rosa H, Robson SC, Sylvestersen KB, Nelson CJ, Nielsen ML, et al. Glutamine methylation in histone H2A is an RNA-polynerase-I-dedicated modification. Nature. 2014;505:564–8.
43. Xing YH, Yao RW, Zhang Y, Guo CJ, Jiang S, Xu G, et al. SLERT regulates DDX21 rings associated with Pol I transcription. Cell. 2017;169:664–78.
44. Deng W, Lopez-Camacho C, Tang JY, Mendoza-Villanueva D, Maya-Mendoza A, Jackson DA, et al. Cytoskeletal protein filamin A is a nucleolar protein that suppresses ribosomal RNA gene transcription. Proc Natl Acad Sci USA. 2012;109:1524–9.
45. Wang J, Zhao S, Wei Y, Zhou Y, Shore P, Deng W. Cytoskeletal filamin A differentially modulates RNA polymerase III gene transcription in transformed cell lines. J Biol Chem. 2016;291:25239–46.
46. Peng F, Zhou Y, Wang J, Guo B, Wei Y, Deng H, et al. The transcription factor Sp1 modulates RNA polymerase III gene transcription by controlling BRF1 and GTF3C2 expression in human cells. J Biol Chem. 2020;295:4617–30.
47. Yin X, Zhang K, Wang J, Zhou X, Zhang C, Song X, et al. RNA polymerase I subunit 12 plays opposite roles in cell proliferation and migration. Biochem Biophys Res Commun. 2021;560:112–8.
48. Cardiff RD, Miller CH, Munn RJ. Manual hematoxylin and eosin staining of mouse tissue sections. Cold Spring Harb Protoc. 2014;2014:655–8.
49. Canene-Adams K. Preparation of formalin-fixed paraffin-embedded tissue for immunochemistry. Methods Enzymol. 2013;33:225–33.
50. Zhang C, Zhao H, Song X, Wang J, Zhao S, Deng H, et al. Transcription factor GATA4 drives RNA polymerase III-directed transcription and transformed cell proliferation through a filamin A/GATA4/SP1 pathway. J Biol Chem. 2022;298:101581.
51. Bian Z, Ji W, Xu B, Huo Z, Huang H, Huang J, et al. Noncoding RNAs involved in the STAT3 pathway in glioma. Cancer Cell Int. 2021;21:445.
52. Filppu P, Tanjore Ramanathan J, Granberg KJ, Gucciardo E, Haapasalo H, Lehti K, et al. CD109-GP130 interaction drives glioblastoma stem cell plasticity and chemoresistance through STAT3 activity. JCI Insight. 2021;6:e141486.
53. White RJ. RNA polymerases I and III, non-coding RNAs and cancer. Trends Genet. 2008;24:622–9.
54. Szakács G, Paterson JK, Ludwig JA, Booth-Genthe C, Gottesman MM. Targeting multidrug resistance in cancer. Nat Rev Drug Disco. 2006;5:219–34.
55. Unsoy G, Gunduz U. Smart drug delivery systems in cancer therapy. Curr Drug Targets. 2018;19:202–12.

AUTHOR CONTRIBUTIONS

CZ performed most work in Figs. 1–8 and in the supplementary file; JW validated data and mentored researchers; YS and DY performed cell culture and cell line screening; YP and BG performed gene cloning; HD prepared CRPSR dCas9 expression system, designed experiments and performed a part of supervision work; XY performed RPA34 shRNA cloning; SZhang and SZhao performed most of the supervision work, processed data, and edited the manuscript; WD acquired the fund of this work, designed experiments, processed data, and wrote the manuscript.

FUNDING

This work was funded by the National Natural Science Foundation of China (31671357 to WD, 62172312 to SZhang).

COMPETING INTERESTS

The authors declare no competing interests.

ETHICS APPROVAL AND CONSENT TO PARTICIPATE

Animal experiments were approved by the Animal and Medical Ethics Committee of School of Life Science and Health at Wuhan University of Science and Technology. The animal protocols abided by the Animal Welfare Guidelines (China).

ADDITIONAL INFORMATION

Supplementary information The online version contains supplementary material available at https://doi.org/10.1038/s41416-022-02098-6.

Correspondence and requests for materials should be addressed to Shasha Zhao, Huan Deng, Shihua Zhang or Wensheng Deng.

Reprints and permission information is available at http://www.nature.com/reprints

Publisher's note Springer Nature remains neutral with regard to jurisdictional claims in published maps and institutional affiliations.